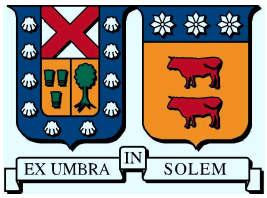

Universidad Técnica Federico Santa María
Departamento de Física

Pion Production by Diffraction of W Bosons in the Dipole Model

Autor: Daniel Egaña Ugrinovic
Trabajo de tesis presentado como requisito parcial para optar al grado de Magíster en Ciencias, Mención Física.

Profesor Guía: Iván Schmidt Andrade
Junio de 2011.

Pion Production by Diffraction of W Bosons in the Dipole Model

Approved by supervising committee:

Supervised by:

Marcelo Loewe: _____

Boris Kopeliovich: _____

Iván Schmidt: _____

Abstract:

In this work the scattering of neutrinos off heavy nuclei by exchange of W bosons in the color dipole model is studied, for small boson virtualities and energies of the order of some GeV's. The first objective of this work is to analyze the black disc limit and to compare the results of the dipole model using perturbative light front wave functions with the ones of the meson model, which are vanishing because of lepton current conservation. Since both results differ, a more complete analysis is carried out, based on Glauber's approach.

At high energies, it is known that the color dipole model is well suited to study diffractive processes on nuclei, but at smaller energies the dipole lifetime is not large enough for the dipole to travel through the nucleus with a frozen transverse size. The short-lived dipoles are identified, and explicit calculations are carried out to determine if they have a large contribution to the final cross section. Although the model presents serious problems because of these short-lived asymmetric pairs, it provides a lower bound for the total cross section of pion production and it gives some additional hints that could be also of interest in more sophisticated models.

Keywords: diffraction, color dipole model, pion production, Glauber's formalism, eikonalization, black disc limit, lifetime, light cone wave functions.

Contents

1 Introduction

It is well known that at high energies and high boson virtualities, several perturbative approaches can be used to study deep inelastic scattering of leptons off nucleons or nuclei. There is plenty of literature concerning this kinematical region, and many of the involved processes are very well understood. However, the literature describing the kinematical region of low Q^2 and high ν is much more scarce, and new processes could arise in this region.

With this motivation, in this work the diffractive production of pions by charged current interactions is studied. This process is commonly analyzed in the low Q^2 (less than $1[GeV]$) and moderately high ν (of the order of some $GeV's$) regime by using meson models [1] [2]. These models, at least in the simplest case, the black disc limit, predict that the process is forbidden in the chiral limit due to lepton current conservation. However, there are alternatives to the meson model.

At high ν and Q^2, the color dipole model has been very successful in describing several diffractive processes [3]. The model can also be used for small values of Q^2, as small as the constituent quark masses m_q [4]. For this reason, an approach based on this formalism and Glauber's theory for scattering on nuclei is a valid alternative to the meson description, as long as the lifetime of the dipole is long enough for its transverse size to remain frozen as it travels through the nuclear matter. Then, pion diffractive production in the scattering of neutrinos off nuclei by charged currents at high ν and low Q^2 (process depicted in figure 2.1) can be analyzed in the context of the color dipole model. The case of heavy nuclei is studied, as this case should be the closest to the black disc limit.

In section 2 the basic mathematical framework and notation is introduced, and a brief outline of the problem is presented. In section 3 a description of the diffraction formalism and the basics of both the meson and the color dipole models is given. The analysis and results for the meson model are well known [2], so only some brief comments on this approach are given, and the attention is focused on the dipole model, which is described in detail in section 3.3. In the end of section 3, the kinematical region of validity of the analysis and the potential problems that could arise in the treatment are discussed.

The results for the dipole model are given in section 4. First, the perturbative wave functions of both the W boson and the scalar pion are presented. Next, the vanishing contributions of the vector current and the transverse parts of the axial current are analyzed, and the non-vanishing longitudinal axial current contribution are studied in two cases: the black disc limit and the scattering on heavy nuclei. For the latter case, a phenomenological dipole cross section and Glauber's approximation for multiple scattering are used, and the scattering of the W boson off the nucleus is first presented, to proceed later to a detailed discussion of the total process (including the leptonic current). The results show that a detailed analysis of the dipole lifetime has to be taken into account, as asymmetric pairs (with light cone fraction z near 0 or 1) tend to have a very short lifetime, so they cannot be treated by the frozen dipole approximation and Glauber's approach. This analysis is carried out, and the contributions of the "problematic" dipoles, *i.e.*, the dipoles with very short lifetimes, are singled out, to test the accuracy of the model. The results show that the error of the calculations increase with decreasing energy ν, so that they are only reliable at energies larger than $20[GeV]$. These results are discussed in the conclusions, where some additional remarks on why the meson model could be making wrong predictions in the black disc limit are also given.

Most of the theoretical framework is presented in the form of appendixes at the end of this document, including a derivation of the color dipole model by using a mixed approach based on light cone quantization rules and loop integrals over the minus component of the momenta, and a rather complete description of Glauber's theory.

2 Basics

The main task of this work is to to calculate and analyze the scattering amplitude of the process depicted in figure 2.1, where neutrinos scatter off nuclei of mass m_N, and produce a final scalar pion and a lepton. We neglect all the lepton masses and we constrain the analysis to the case where the nucleus scatters elastically, *i.e.*, it maintains its original mass. The scattering amplitude is given by (we follow a similar notation as the one found in [1])

$$\mathcal{M} = \frac{g_W}{m_W^2} l^\mu h_\mu, \tag{2.1}$$

where l^μ and h^μ are the leptonic and hadronic currents, respectively, and $\frac{G_F}{\sqrt{2}} = \frac{g_W^2}{m_W^2}$. One of the powers of g_W is absorbed in the hadronic current, in contrast to the convention used in [1], where g_W appears squared in 2.1.

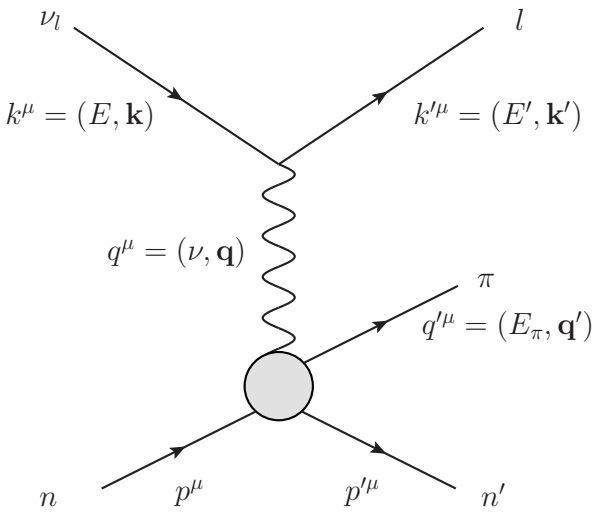

$\nu = E - E'$

$q^2 = -Q^2$

$t = (q' - q)^2$

$s = (k + p)^2$

$s' = (q + p)^2$

$q'^2 = m_\pi^2$

$p^2 = p'^2 = m_N^2$

Figure 2.1: **Production of charged pions**

The leptonic current is given by

$$l^\mu = \bar{l}(k')\gamma_\mu(1 - \gamma_5)\nu(k)\,, \tag{2.2}$$

so that squared and averaged over initial spins, it gives the leptonic tensor

$$L_{\mu\nu} = 2k_\mu k_\nu - k_\mu q_\nu - q_\mu k_\nu + (k \cdot q)g_{\mu\nu} - i\varepsilon_{\mu\nu\rho\sigma}k^\rho q^\sigma\,. \tag{2.3}$$

This leptonic tensor can be used to express the unpolarized squared scattering amplitude as

$$|\mathcal{M}|^2 = \left(\frac{g_W}{m_W^2}\right)^2 L^{\mu\nu} h_\mu h_\nu^*\,. \tag{2.4}$$

Let's recall the general expression for the differential cross section for a two particle scattering process

$$d\sigma = \frac{1}{\phi}|\mathcal{M}|^2 d\Pi_n\,, \tag{2.5}$$

where ϕ is the flux of incident particles and $d\Pi_n$ is the phase space differential. In our case, we have

$$\begin{aligned}\phi &= 2\sqrt{\lambda(s,0,m_N^2)}\,,\\ d\Pi_3 &= \frac{d^3\mathbf{k}'}{(2\pi)^3}\frac{1}{2E'}\frac{d^3\mathbf{q}'}{(2\pi)^3}\frac{1}{2q_0'}\frac{d^3\mathbf{p}'}{(2\pi)^3}\frac{1}{2p_0'}(2\pi)^4\delta(k'+q'+p'-k-p)\,,\end{aligned} \tag{2.6}$$

where $\lambda(x,y,z) = x^2+y^2+z^2-2xy-2xz-2yz$ is the triangle function. By counting the energy-momentum conservation equations, on-shell conditions and other constrains on the kinematical variables, it is easy to see that the process has only 5 independent variables, in addition to the incident energy of the neutrino, E. We take this variables to be (ν, t, Q^2) and the azimuthal angles of scattering of the final lepton and the pion. The analysis is greatly simplified by noticing that the process has no dependence whatsoever on these last two angles (our model for the scattering amplitude will not depend on them, see sec. 3), so we can easily integrate over the angles, and after some algebraic work we obtain,

$$\frac{d\sigma}{dQ^2 d\nu dt} = \frac{1}{(2\pi)^3}\frac{\left(4m_N^2|\mathbf{q}'|^2 - t(t+Q^2-m_\pi^2) - 2\nu m_N(t+m_\pi^2+Q^2)\right)\sqrt{\nu^2+Q^2}}{96 m_N^2 E^2 |\mathbf{q}'|^2 \lambda(s',q^2,m_N^2)}|\mathcal{M}|^2\,, \tag{2.7}$$

where $|\mathbf{q}'|$ as a function of t, ν and Q^2 is given by

$$|\mathbf{q}'| = \frac{1}{2m_N}\sqrt{4m_N^2(\nu^2-m_\pi^2)+t^2+4t\nu m_N}\,. \tag{2.8}$$

The challenging part of the analysis is of course to find a model able to describe correctly the scattering of virtual W bosons off nuclei (a model for the hadronic current). We can then concentrate on this part, and study the virtual W boson - nuclei scattering process depicted in figure 2.2, with amplitude

$$\mathcal{M}_h = \varepsilon^\mu(\nu,\mathbf{q})h_\mu\,, \tag{2.9}$$

where ε is the polarization vector of the virtual boson. Note that we can expand h^μ in terms of a complete set of four vectors. This will be very useful to obtain h^μ from the scalar, longitudinal and transverse part of $\mathcal{M}_h$ that we will call $c_S, c_L, c_{\pm1}$ respectively. We can take this set to be the momenta of the W boson, and its three polarization vectors,

$$h^\mu = c_S\frac{q^\mu}{Q} + c_L\varepsilon_L^\mu + c_1\varepsilon_1^\mu + c_{-1}\varepsilon_{-1}^\mu\,. \tag{2.10}$$

We will work in the reference frame where the boson momentum lies on the z axis, so that its momentum and polarization vectors are given by

$$\begin{aligned} q &= (\nu,\mathbf{0},\sqrt{\nu^2+Q^2}),\\ \varepsilon_L &= \frac{1}{|Q|}(\sqrt{\nu^2+Q^2},\mathbf{0},\nu),\\ \varepsilon_{\pm1} &= -\frac{1}{\sqrt{2}}(0,1,\pm i,0).\end{aligned} \tag{2.11}$$

Note that for the scattering of real W bosons the scalar part c_S of h^μ is completely unimportant, as there are no scalar bosons. On the other hand, for our virtual process 2.1, the scalar part can give some contributions, but in the chiral limit they vanish because of current conservation, $q^\mu l_\mu = 0$. The cross section for the process 2.9 is given by

$$\frac{d\sigma}{dt} = \frac{1}{16\pi\lambda(s',q^2,m_N^2)}|\mathcal{M}_h|^2\,, \tag{2.12}$$

where m_N the mass of the target. The triangle function reduces to s' when we neglect the boson "mass" q^2 and the target mass. Anyway, it should be noted that the factor which multiplies the amplitude squared in 2.12 is somewhat arbitrary, because we cannot measure the flux of virtual W bosons. There are different conventions to define this flux, and here we take it to be the flux that a W boson with mass q^2 would have.

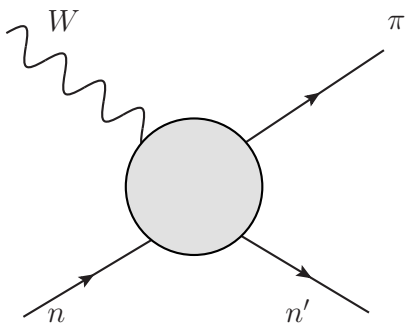

Figure 2.2: **Hadronic part**

There are two options to analyze the hadronic current, which we will discuss in the following section. The common understanding is that both should give the same results, but as it will be shown, this is not the case, and we will give some hints to explain the origin of this difference.

3 Models for pion diffractive production

3.1 Introduction: diffraction in high energy scattering

The first use of the concept of diffraction in relativistic scattering theory was formulated by Good and Walker in 1960 [5]. The idea is actually very simple, and it was taken from classical electrodynamics and non relativistic quantum mechanics. A diffractive process is a high energy process, where the final particle acquires a component that corresponds to one of the terms of the virtual dissociation of the incident particle. A typical example of this processes comes from optics. If a plane wave, let's say polarized along the x axis, passes through a polarizing plane which has a polarization axes forming a 45^{o} angle with the x axis, we obtain in the final "state", a wave that has components with polarization along both the x and the y axis. Notice that not only the final state has elements of the initial one, but also it acquired a component that is orthogonal to the initial state, so this is also a possibility in diffractive processes.

In field theoretical terms, *diffractive processes of hadrons* are by definition, *high energy processes in which no quantum numbers are exchanged*. Isospin, charge, strangeness, color and other quantum numbers must be conserved, but spin can change because angular momentum can be transferred in the collision. Then, for example, one gluon exchange processes cannot be diffractive because they exchange color, but two gluon exchange processes can. Diffraction is characterized also by a large rapidity gap between the initial and final state. This characteristic is useful to provide an operative definition for diffraction, that allows us to discern between diffractive and non diffractive processes. For a detailed discussion see [3].

If we have a scattering process where a state $|\gamma\rangle$ (a particle) interacts with a target $|N\rangle$ (a nucleus, for example), we have two alternatives: either the state $|\gamma\rangle$ scatters *elastically* into itself, $|\gamma\rangle \to |\gamma\rangle$ or it scatters *diffractively* into another state $|\gamma\rangle \to |\rho\rangle$. Here we have warn the reader to avoid confusions: this names could be misleading because *both* processes are diffractive, as they don't exchange quantum numbers. γ and ρ are defined uniquely by specifying the kind of particle (or particles in the case of a multiparticle state, as a color dipole) we are talking about, and a set of quantum numbers (as momenta and helicities).

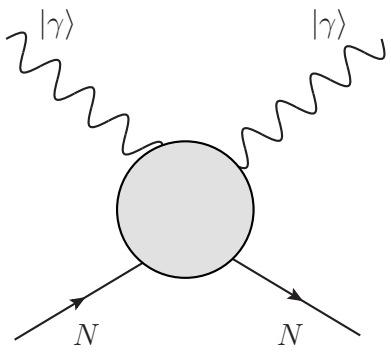

Figure 3.1: **Elastic scattering**

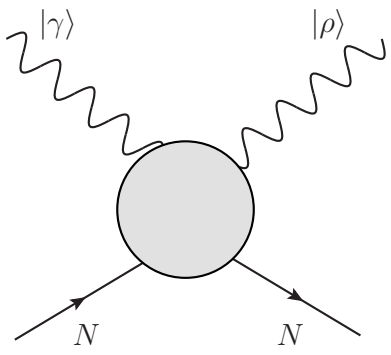

Figure 3.2: **Diffractive scattering**

In both processes we are assuming that the target does not take part in the scattering process, i.e., it just plays the role of some kind of obstacle that facilitates the diffractive process of the projectile. The target particle will not be observed by the detectors, so the attention should be focused in the diffractive process of the projectile. For this reason, we can forget about the target for a moment, and just introduce a *diffraction operator* $\hat{D}$

which gives the amplitude for diffractive scattering

$$D_{ik} = \langle k \mid \hat{D} \mid i \rangle \,, \tag{3.1}$$

where $|i\rangle$ is the initial state of the projectile, and $|k\rangle$ the final particle. The main difference between the regular time evolution operator and the diffraction operator (also called diffraction matrix), is that the dependence of the process on the target particle is fully contained in the latter. If the target particle is excited or acquires momentum during the scattering process, that information has to be included also in the diffraction matrix.

If the particle scatters elastically we say it is a *diffraction eigenstate*, $|\alpha\rangle$, so that

$$\hat{D} \,|\alpha\rangle = i d_{\alpha N} \,|\alpha\rangle \ . \tag{3.2}$$

To simplify the treatment, the assumption that the diffraction eigenvalues are purely imaginary can be made. This assumption can be understood by using the optical theorem. The total cross section increases at higher energies, because at higher the energy more final states can be produced. As the imaginary part of the elastic amplitude is proportional to the center of mass energy times the total cross section, it also increases with energy. No such constrain exists on the real part of the scattering amplitude, so the ratio of the real part to the imaginary part of the forward scattering amplitude should decrease with energy. A detailed analysis and experimental results, show that this reasoning is indeed correct, and at energies of the order of some GeV's the ratio between the real and imaginary part of the forward scattering amplitude is smaller than 0.1 ([3]).

Then, using the optical theorem we can express the amplitudes d_α in terms of the total scattering cross section σ_α,

$$\sigma_{\alpha N} = \frac{1}{\sqrt{\lambda(s, m_\alpha^2, m_N^2)}} d_{\alpha N} \,, \tag{3.3}$$

where $\lambda(x, y, z)$ is the triangle function, s is the total c.m. energy and m_α, m_N are the masses of the projectile and target, respectively. To study the scattering of a general projectile $|i\rangle$ we can expand it in terms of diffraction eigenstates,

$$|i\rangle = \sum_\alpha c_{i\alpha} \,|\alpha\rangle \ . \tag{3.4}$$

The coefficients $c_{i\alpha}$ are the *wave functions* that give us the decomposition of the projectile i in terms of diffraction eigenstates α. In this way, it is easy to see that any diffraction matrix element can be obtained in terms of the wave functions and the elastic scattering amplitude of the scattering eigenstates,

$$D_{ik} = \langle k \mid \hat{D} \mid i \rangle = \sum_\alpha c_{k\alpha}^* c_{i\alpha} d_{\alpha N} \,. \tag{3.5}$$

In particular, the elastic scattering element D_{ii} is

$$D_{ii} = \sum_\alpha |c_{i\alpha}|^2 d_{\alpha N} \,, \tag{3.6}$$

and using the optical theorem, the total iN scattering cross section is

$$\sigma_{iN} = \frac{1}{\sqrt{\lambda(s, m_i^2, m_N^2)}} D_{ii} = \sum_\alpha \frac{\sqrt{\lambda(s, m_\alpha^2, m_N^2)}}{\sqrt{\lambda(s, m_i^2, m_N^2)}} |c_{i\alpha}|^2 \sigma_{\alpha N} \,. \tag{3.7}$$

If s and m_N are much greater than the masses of the projectiles m_α and m_i, the result is simplified to the one found in the literature [3],

$$\sigma_{iN} = \sum_\alpha |c_{i\alpha}|^2 \sigma_{\alpha N} \,. \tag{3.8}$$

From this last expression or from expression 3.5 we see that the problem is divided into two parts, provided that we already identified the diffraction eigenstates α:

1. To find the wave functions of the initial and final states $|k\rangle$ and $|i\rangle$ and expand them in terms of diffraction eigenstates.

2. To find the total scattering cross section $\sigma_{\alpha N}$ of diffraction eigenstates $|\alpha\rangle$.

If we are able to solve these two problems, we will have a model which correctly describes the diffraction process. But even if this formalism has been very successful ([6]) each problem has its difficulties, even if we correctly identified the diffraction eigenstates. First, it is not always easy to find the wave functions of the projectile and final particle. In the high energy limit, we can resort to a perturbative treatment that give us a good model for the wave functions, but non perturbative effects appear at low virtualities of the projectile (when the projectile is a virtual particle). Additionally, if the projectile is a compound particle, as in the hadron case, it is not possible to calculate exactly the wave function and we have to use models that introduce uncertainty into the treatment.

Second, although there has been much success in modeling the scattering amplitude of the diffraction eigenstates by using a universal phenomenological cross section (by universal it is understood that the cross section is the same regardless of the analyzed process), there are still some uncertainties in these models, especially for small virtualities of the projectile, where perturbative calculations as the two gluon exchange approximation, are not valid.

Now, as regards to the diffraction eigenstates, it was first identified by Zamolodchikov and Kopeliovich in [9] that the color dipole (a quark antiquark pair) of definite transverse size scatters elastically in nuclear matter. Here, the term diffraction eigenstate is used somewhat loosely, because the transverse size of the dipole remains frozen and no new particles are created (the final particle is also a color dipole) but other quantum numbers as the transverse center of mass momentum may change, as depicted in figure 3.3. We will address this model in detail in section 3.3.

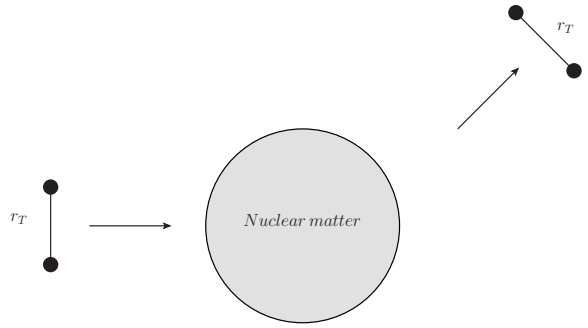

Figure 3.3: **The transverse size of the dipole remains frozen, but the transverse c.m. momentum may change**

To end this section, it is important to note one last subtlety: the diffraction eigenstates are *states on the light-front*. That means that they are states defined and evolved at fixed light cone time, and that the wave functions are *light-cone wave functions*. Actually, the projectile itself is also a state defined on the light cone, in contrast to the usual states used in most text books where they are defined at a fixed regular time [7]. But why are we using these light-cone states? Qualitatively, the question can be answered by thinking what does the target (and the laboratory rest frame) sees. At low energies, the projectile

travels slowly, so that the information that it send us reach us very fast and we can see its instantaneous motion.

At high energies, the target sees the information that a projectile traveling at the speed of light sends. This information is sent in light-fronts, just in the same way as the information that we receive from a classical wave is received in wave fronts. For this reason, it is reasonable to expect that light-cone states should be the adequate basis to describe the process. A formal approach based in light-cone quantization rules gives the same conclusions. A discussion of the color dipole model in relation with light-cone quantization rules is given in 6.1.3.

3.2 Meson model

The first alternative to describe the hadronic current is to use a meson model [1], as in figure 3.4 where the W boson fluctuates into mesons, and by diffraction, a final charged pion is produced. If the W boson is expressed as a sum over all the possible meson states $\langle\xi|$,

$$|W\rangle = \sum_{\xi} \Psi_{\xi} \, |\xi\rangle \ , \tag{3.9}$$

then, the scattering amplitude is given by the diffraction matrix $\hat{D}$,

$$\mathcal{M}_h = \langle \pi \mid \hat{D} \mid W \rangle \, . \tag{3.10}$$

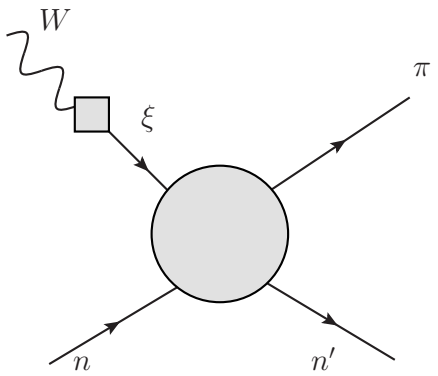

Figure 3.4: **Scattering of a virtual W boson in the meson model**

The coefficients Ψ_{ξ} can be calculated by studying how the W boson couples to the corresponding meson field. For the moment, in our analysis of $\mathcal{M}_h$ we will stick to the simplest case, the black disc limit. In this limit, valid for heavy nuclei, the scattering amplitude or diffraction matrix $\hat{D}$ for a hadron that scatters off nuclei is just a constant in impact parameter space. This means that if we expand the mesons in 3.9 as a sum in Fock space over its inner constituents, each Fock state scatters equally, and therefore the whole meson wavefunction is just multiplied by a constant after the scattering. No inelastic transitions are allowed, and the scattering amplitude reduces to

$$\mathcal{M}_h \propto \langle W|\pi\rangle = \Psi_{\pi} \, . \tag{3.11}$$

If we use an effective Lagrangian theory to describe the scalar pion - W boson interaction, it is easy to see that in the Lagrangian, the pion field π can be coupled to the W boson field W^{μ} only through terms of the form $\partial_{\mu}\pi W^{\mu}$. Then, in perturbation theory, the

polarization vector of the W boson couples to the pion only through a term proportional to q^μ [2]. For this reason, in equations 2.9 and 2.10, c_S is the only non-vanishing coefficient of the expansion, so we have

$$h^\mu \propto q^\mu \,. \tag{3.12}$$

Then, using 2.1 we obtain

$$\mathcal{M} \propto l^\mu q_\mu = 0 \,, \tag{3.13}$$

because of lepton current conservation (up to small terms of order m_{lepton}/ν).

3.3 Dipole model

The second alternative is to use the color dipole model [8], which is valid for high energies and low values of Bjorken's variable x. In this model, depicted in figure 3.5, the W boson fluctuates into an on-shell quark-antiquark pair, which scatters off the nucleus and then forms the final pion. The main observation is that this color dipole is an interaction eigenstate at high energies so the transverse separation of the dipole during the scattering process is frozen [9]. Nonetheless, its light-cone momentum must change, in order to satisfy light-cone momentum conservation at the vertex where the final pion is formed. It is worth noting that this formalism is derived from light-cone perturbation theory [10], so each intermediate state is on shell, and only transverse and light-cone momentum are conserved at each vertex (see also the notes in section 3.1). The minus component of each momentum is not conserved, and is obtained by the aforementioned on-shell condition. For a detailed derivation of the model in light-cone perturbation theory, see appendix 6.1.

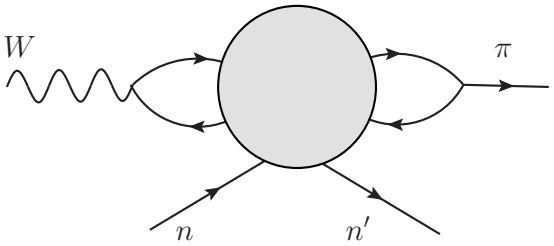

Figure 3.5: **Scattering of a virtual W boson in the dipole model**

To calculate the scattering amplitude of the process, we can now expand both the W boson and the pion in terms of dipoles of different transverse and light-cone momenta,

$$|W\rangle = \sum_{\lambda_1,\lambda_2} \int dz d^2k_T \Psi^W_{q\bar{q}}(\mathbf{k_T}, z, Q^2, q^+, \lambda_1, \lambda_2) \left|q\bar{q}(\mathbf{k_T}, z, q^+, \lambda_1, \lambda_2)\right\rangle \,, \tag{3.14}$$

where the momenta of the W boson, quark and antiquark in the light-cone notation are given by

$$\begin{aligned} q &= (q^+, -\frac{Q^2}{q^+}, \mathbf{0}) \,, \\ p_1 &= (zq^+, \frac{\mathbf{k}_T^2 + m_q^2}{zq^+}, \mathbf{k_T}) \,, \\ p_2 &= ((1-z)q^+, \frac{\mathbf{k}_T^2 + m_{\bar{q}}^2}{(1-z)q^+}, -\mathbf{k_T}) \,, \\ 0 &\leq z \leq 1 \,. \end{aligned} \tag{3.15}$$

$\Psi^W_{q\bar{q}}$ is the W boson wave function, also called distribution amplitude (because it is not normalized), and λ_1, λ_2 are the polarization of the quark and antiquark, respectively. Note also that we are working in the reference frame where the W boson has no transverse momentum. The axial part of the wave function of the W boson is given in terms of the spinors and gamma matrices by (see app. 6.1)

$$\Psi^{W_A}_{q\bar{q}}(\mathbf{k_T}, z, Q^2, q^+, \lambda, \lambda_1, \lambda_2) = \sqrt{N_c} g_W \frac{\varepsilon^\mu_\lambda(Q)\bar{u}_{\lambda_1}(p_1)\gamma_\mu\gamma_5 v_{\lambda_2}(p_2)}{\sqrt{p_1^+}\sqrt{p_2^+}\left(q^- - p_1^- - p_2^-\right)} = \varepsilon^\mu_\lambda(Q) a_\mu \,, \quad (3.16)$$

and the vector part is given by

$$\Psi^{W_V}_{q\bar{q}}(\mathbf{k_T}, z, Q^2, q^+, \lambda_1, \lambda_2, \lambda) = \sqrt{N_c} g_W \frac{\varepsilon^\mu_\lambda(Q)\bar{u}_{\lambda_1}(p_1)\gamma_\mu v_{\lambda_2}(p_2)}{\sqrt{p_1^+}\sqrt{p_2^+}\left(q^- - p_1^- - p_2^-\right)} = \varepsilon^\mu_\lambda(Q) v_\mu \,, \quad (3.17)$$

where ε_λ the polarization vector of the W boson. The total wave function of the W boson $\Psi^W_{q\bar{q}}$ is the difference between the vector and axial part, but we will see in section 4.3 that the vector part gives no contribution to our process.

In the same way, we can write the pion as,

$$|\pi\rangle = \sum_{\lambda_1', \lambda_2'} \int dz' d^2k_T' \Psi^\pi_{q\bar{q}}(\mathbf{k_T'}, \mathbf{\Delta}, z', m_\pi^2, q'^+, \lambda_1', \lambda_2') \left|q\bar{q}(\mathbf{k_T'}, \mathbf{\Delta}, z', q'^+, \lambda_1', \lambda_2')\right\rangle \,, \quad (3.18)$$

where the momenta of the charged pion, quark and antiquark are given by

$$\begin{aligned} q' &= (q'^+, -\frac{m_\pi^2}{q'^+}, \mathbf{0}) \,, \\ p_1' &= (z'q'^+, \frac{(\mathbf{k_T'} + \mathbf{\Delta})^2 + m_q^2}{z'q'^+}, \mathbf{k_T'} + z\mathbf{\Delta}) \,, \\ p_2' &= ((1-z')q'^+, \frac{(\mathbf{k_T'} + \mathbf{\Delta})^2 + m_{\bar{q}}^2}{(1-z')q'^+}, -\mathbf{k_T'} + (1-z)\mathbf{\Delta}) \,, \\ &0 \leq z' \leq 1 \,. \end{aligned} \quad (3.19)$$

We will couple the pion to the quark-antiquark pair using an effective Lagrangian theory through the simplest possible vertex: a constant multiplied by a γ_5 matrix. In this way, the pion WF is

$$\Psi^\pi_{q\bar{q}}(\mathbf{k_T'}, \mathbf{\Delta}, z', m_\pi^2, q'^+, \lambda_1', \lambda_2') = c_\pi \frac{\bar{u}_{\lambda_1'}(p_1')\gamma_5 v_{\lambda_2'}(p_2')}{\sqrt{p_1'^+}\sqrt{p_2'^+}\left(q'^- - p_1'^- - p_2'^-\right)} \,. \quad (3.20)$$

The transferred transverse momentum does not play any role in the wave functions, because they are independent of this parameter. This makes sense, because the decomposition of a particle in terms of dipoles has to be independent of the direction in which the particle moves. Taking the inner product in 3.10 we obtain

$$\begin{aligned} \mathcal{M}_h = \sum_{\lambda_1, \lambda_2, \lambda_1', \lambda_2'} \int d^2\mathbf{k_T} d^2\mathbf{k_T'} dz dz' \\ \left(\Psi^\pi_{q\bar{q}}(\mathbf{k_T'}, \mathbf{\Delta}, z', m_\pi^2, q'^+, \lambda_1', \lambda_2')\right)^* \Psi^W_{q\bar{q}}(\mathbf{k_T}, z, Q^2, q^+, \lambda_1, \lambda_2, \lambda) \\ \langle q\bar{q}(\mathbf{k_T'}, \mathbf{\Delta}, z', q'^+, \lambda_1', \lambda_2') \mid \hat{D} \mid q\bar{q}(\mathbf{k_T}, z, q^+, \lambda_1, \lambda_2)\rangle \quad . \end{aligned} \quad (3.21)$$

Now, we have to discuss about what information does the color dipole model give us to simplify the treatment. The dipole model tell us that at high energies the dipole is

an interaction eigenstate, so that its transverse size remains frozen during the scattering process, as depicted in fig. 3.3. Then, the diffraction matrix cannot change the dipole's transverse size (we understand by "transverse size", the size of the dipole in the plane orthogonal to the direction of its movement), but has to provide the transition to dipoles with different light-cone momenta (because $q_+ \neq q'_+$) and helicities. The most general expression for these conditions to be fulfilled is

$$\hat{D}\left|q\bar{q}(\mathbf{r_T}, z, q^+, \lambda_1, \lambda_2)\right\rangle = \sum_{\lambda''_1,\lambda''_2} \int dq''_+ dz'' \mathcal{A}(r_T, q_+, q''_+, z, z'', \lambda_1, \lambda_2, \lambda''_1, \lambda''_2) \left|q\bar{q}(\mathbf{r_T}, z'', q^+, \lambda''_1, \lambda''_2)\right\rangle , \tag{3.22}$$

where $\mathcal{A}$ is the dipole scattering amplitude and

$$\left|q\bar{q}(\mathbf{r_T}, z, q^+, \lambda_1, \lambda_2)\right\rangle = \int d^2\mathbf{k_T} \exp\left(i\mathbf{k_T}\cdot\mathbf{r_T}\right) \left|q\bar{q}(\mathbf{k_T}, z, q^+, \lambda_1, \lambda_2)\right\rangle . \tag{3.23}$$

Now, using eqs. 3.21, 3.22, 3.23 and noting that dipoles with different values of $\mathbf{r_T}$, z, q_+ or helicities are orthogonal, we end up with

$$\mathcal{M}_h = \frac{1}{4\pi} \sum_{\lambda_1,\lambda_2,\lambda'_1,\lambda'_2} \int d^2\mathbf{r_T} dz dz' \Psi^*_\pi(\mathbf{r_T}, z', m^2_\pi, q'_+, \lambda'_1, \lambda'_2)\Psi_W(\mathbf{r_T}, z, Q^2, q_+, \lambda_1, \lambda_2, \lambda)\mathcal{A}(r_T, q_+, q'_+, z, z', \lambda_1, \lambda_2, \lambda'_1, \lambda'_2) , \tag{3.24}$$

where we dropped the subindex $q\bar{q}$ in the wavefunctions, as from now on, functions denoted by the letter Ψ will always refer to color dipole wavefunctions. We will also write $\mathbf{r_T}$ or $\mathbf{k_T}$ in the argument of the wavefunctions, depending if we are using the WF in momentum or configuration space (they are related by a simple Fourier transform). The prefactor $\frac{1}{4\pi}$ is due to the convention used for the wave functions (see [11] and 4.2.1).

The result obtained in 3.24 is the most general that one can obtain for the color dipole model. In Glauber's approach for multiple scattering on nuclei the helicities of the $q\bar{q}$ pair and the fractions of the light-cone momentum z are conserved, and the elastic scattering amplitude is (see [3], [12] and especially 6.2)

$$\begin{aligned}\mathcal{A}(r_T) &= 2\sqrt{\lambda(s', q^2, m^2_N)} \int d^2\mathbf{b} \exp(i\mathbf{\Delta}\cdot\mathbf{b}) \left(1 - \exp\left(-\frac{1}{2}\sigma^p_{q\bar{q}}(\mathbf{r_T})T(b)\right)\right) \\ &= 4\pi\sqrt{\lambda(s', q^2, m^2_N)} \int bdbJ_0(\Delta b) \left(1 - \exp\left(-\frac{1}{2}\sigma^p_{q\bar{q}}(\mathbf{r_T})T(b)\right)\right) ,\end{aligned} \tag{3.25}$$

where $\sigma^p_{q\bar{q}}$ is the dipole scattering cross section on nucleons, $T(b)$ the nucleus profile function, λ the triangle function and Δ^2 is the transverse transferred momentum squared. In the high s' limit, and neglecting terms of the order Q^2/m^2_N and m^2_π/m^2_N, we obtain $\Delta^2 = -t$, either in the CM reference system or the Lab system (our case), because the transverse momentum is invariant under boosts along the longitudinal axis. With these assumptions we obtain

$$\mathcal{M}_h = \frac{1}{4\pi} \sum_{\lambda_1,\lambda_2} \int d^2\mathbf{r_T} dz \Psi^*_\pi(\mathbf{r_T}, z, m^2_\pi, q'_+, \lambda_1, \lambda_2)\Psi_W(\mathbf{r_T}, z, Q^2, q_+, \lambda_1, \lambda_2, \lambda)\mathcal{A}(r_T) , \tag{3.26}$$

where N_c is the number of quark colors. At this point, it is easy to see that the hadronic current in the dipole model is given by

$$h^\mu = \frac{1}{4\pi} \sum_{\lambda_1,\lambda_2} \int d^2\mathbf{r_T} dz \Psi^*_\pi(\mathbf{r_T}, z, m^2_\pi, q'_+, \lambda_1, \lambda_2)(a^\mu + v^\mu)\mathcal{A}(r_T) . \tag{3.27}$$

If the nucleus of radius r_N is very dense so that $\sigma^p_{q\bar{q}}(\mathbf{r_T})T(b) >> 1$ for $b < r_N$ and zero otherwise, $\mathcal{A}(\mathbf{r_T}) = constant$, we obtain the black disc limit,

$$\mathcal{M}^{BD}_h \propto \sum_{\lambda_1,\lambda_2} \int dr^2_T dz \Psi^*_\pi(\mathbf{r_T}, z, m^2_\pi, q'_+, \lambda_1, \lambda_2)\Psi_W(\mathbf{r_T}, z, Q^2, q_+, \lambda_1, \lambda_2, \lambda)\,. \qquad (3.28)$$

In section 4.4, we will try to calculate the scattering amplitude in the BD limit and we will see that it diverges for a very simple reason: we are omitting color transparency and this effect is of uttermost importance to eliminate the divergences that arise in the wavefunctions at small $\mathbf{r_T}$.

3.4 Kinematical region

We now elaborate on the regime in which we are working on discussing the relevant kinematical variables. The color dipole model is valid only if the following conditions are met.

- *Bjorken variable x:* we need $x << 1$ so that the virtual boson doesn't strike directly the quarks of the nucleon or nucleus, but it first fluctuates into a $q\bar{q}$ pair, and then scatters off the target by gluon exchange. At high energies, in practice this means $x < 0.02$. This requirement is related to the requirement on the lifetime of the dipole that we will explain below, and at high energies they are equivalent.

- *Quark-antiquark pair lifetime, τ:* the time of scattering must be much less than the quark-antiquark lifetime $\tau \approx \frac{q_+}{Q^2}$. In the two-gluon approximation, this condition reduces to

$$l_+ << \frac{q_+ l^2_T}{Q^2}, \qquad (3.29)$$

  where l is the momentum carried by one of the gluons. This means that q_+ (and therefore the virtual boson energy ν) should be in general much larger than Q^2. We give a very detailed discussion about this requirement in the results section.

- *Boson virtuality, Q^2:* for low Q^2 there are some problems discussed in detail in [13] and especially in [14] (take a look at the conclusions of this last paper). The *"scattering of the dipole"* problem (figure 3.6) is that at low Q^2, the size of the dipole becomes large and non-perturbative effects are introduced in the scattering of the dipole off the target. This means that the simple perturbative treatments like the two-gluon exchange model, loose their ability to describe correctly the scattering of the pair, and we have to modify the dipole scattering cross section for the model to keep its validity. To be more explicit, the problem is that for low Q^2, it is not quite clear which is the form of the dipole cross section. At low virtualities there are higher order perturbative effects, such as the possible rescattering of the quark-antiquark pair off the target, and the fact that the outgoing pion does not couple necessarily to the same dipole loop as the incoming virtual boson. At low Q^2 it is known that the vector meson dominance model applies. Therefore, in this region the aforementioned effects should provide a transition from the dipole model to the meson model.

- *Center of mass energy s:* we are working in the regime of $s \geq 1[GeV]$ and $\nu \geq 1[GeV]$. This is needed because we are neglecting all the lepton masses, but most importantly, because the dipole model is valid only at high energies. The *"model" problem* depicted in figure 3.7, appears when the idea that the dominant contribution to the process comes from a three stage picture (formation of an on shell dipole - scattering of the dipole - formation of the final meson) breaks down. This happens because at lower energies we cannot neglect the instantaneous propagators in the light cone formalism, and the dipoles cannot be put on-shell (see appendix 6.1).

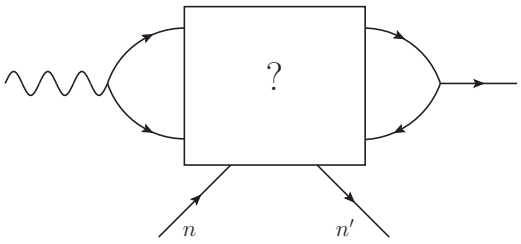

Figure 3.6: **Scattering problem**

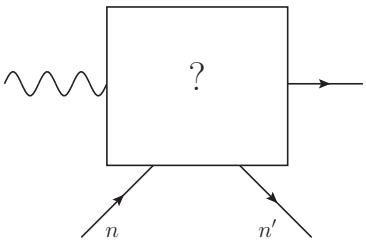

Figure 3.7: **Model problem**

4 Results

4.1 Brief summary of the model

Let us summarize our results until now. Recalling equation 2.10 we have.

$$h^\mu = c_S \frac{q^\mu}{Q} + c_L \varepsilon_L^\mu + c_1 \varepsilon_1^\mu + c_{-1} \varepsilon_{-1}^\mu \,,$$

where the coefficients c_L and $c_{\pm 1}$ are given by (see sec. 3.3)

$$\begin{aligned} c_L &= \frac{1}{4\pi} \sum_{\lambda_1,\lambda_2} \int d^2\mathbf{r_T} dz \Psi_\pi^*(\mathbf{r_T}, z, m_\pi^2, q'_+, \lambda_1, \lambda_2) \Psi_W(\mathbf{r_T}, z, Q^2, q_+, \lambda_1, \lambda_2, \lambda = 0) \mathcal{A}(\mathbf{r_T}) \,, \\ c_{\pm 1} &= \frac{1}{4\pi} \sum_{\lambda_1,\lambda_2} \int d^2\mathbf{r_T} dz \Psi_\pi^*(\mathbf{r_T}, z, m_\pi^2, q'_+, \lambda_1, \lambda_2) \Psi_W(\mathbf{r_T}, z, Q^2, q_+, \lambda_1, \lambda_2, \lambda = \pm 1) \mathcal{A}(\mathbf{r_T}) \,, \end{aligned} \tag{4.1}$$

and the scattering amplitude is given by eq. 3.25

$$\mathcal{A}(r_T) = 4\pi \sqrt{\lambda(s', q^2, m_N^2)} \int b db J_0(\Delta' b) \left(1 - \exp\left(-\frac{1}{2}\sigma_{q\bar{q}}^p(\mathbf{r_T}) T(b)\right)\right) \,.$$

It should be clear by now that the coefficient c_S is unimportant for the process. In the following sections we study and calculate the coefficients c_L and $c_{\pm 1}$. We will see that many contributions to these coefficients vanish, and at the end the numerical efforts will be reduced to calculate only c_L, for different values of Q^2, t and ν.

We will start by giving the expressions for the wave functions and by studying the vanishing contributions to the process. Then, we will analyze the simplest case, the black disc limit, which will be useful to foresee some of the conclusions of the complete analysis. The following step will be to calculate the cross section of diffractive production of pions by virtual W bosons using a phenomenological model, and finally we will include the leptonic current to analyze the total process.

4.2 Wave functions

The wave functions 3.16, 3.17 and 3.20 can be obtained both in transverse momentum and transverse separation space by using the conventions for the spinors and gamma matrices given in the appendix. For the calculations we use Maple and a simple mathematical code. The only subtlety is that the direct calculation of expressions 3.16 and 3.17 gives rise to terms that in configuration space correspond to Dirac deltas centered at zero transverse separation. These terms can be safely removed by hand, because color transparency will eliminate them anyway. We give here the results in matrix notation, where the matrix element (i, j) corresponds to different helicities (λ_1, λ_2). Matrix index 1 means negative helicity, and 2, positive helicity; m and d are the quark and antiquark masses and r_T the magnitude of their transverse separation.

Here, we use the convention for the WF of Kowalsky and Teaney [11], where the WF do not have the prefactor $\frac{1}{\sqrt{4\pi}}$ that is found in part of the literature. In our treatment these factors are included as a factor $\frac{1}{4\pi}$ in 3.26.

4.2.1 W Boson Wave Function

Here, we present the W boson transverse ($\lambda = \pm 1$)and longitudinal ($\lambda = 0$) perturbative WF, both in momentum and configuration space.

In momentum space

Vector Part

$$\Psi^{W_V}_{q\bar{q}}(\mathbf{k_T})\big|_{\lambda=0} = \begin{pmatrix} \frac{c_W(m-d)(k_x+ik_y)}{Q(\mathbf{k_T}^2+a_W^2)} & \frac{-c_W(2Q^2z(1-z)+(m-d)((1-z)m-zd)}{Q(\mathbf{k_T}^2+a_W^2)} \\ \frac{-c_W(2Q^2z(1-z)+(m-d)((1-z)m-zd)}{Q(\mathbf{k_T}^2+a_W^2)} & \frac{c_W(m-d)(-k_x+ik_y)}{Q(\mathbf{k_T}^2+a_W^2)} \end{pmatrix}$$

$$\Psi^{W_V}_{q\bar{q}}(\mathbf{k_T})\big|_{\lambda=1} = \begin{pmatrix} 0 & \frac{c_W\sqrt{2}(z-1)(k_x+ik_y)}{Q(\mathbf{k_T}^2+a_W^2)} \\ \frac{c_W\sqrt{2}z(k_x+ik_y)}{Q(\mathbf{k_T}^2+a_W^2)} & \frac{c_W\sqrt{2}(m(1-z)+dz)}{Q(\mathbf{k_T}^2+a_W^2)} \end{pmatrix}$$

$$\Psi^{W_V}_{q\bar{q}}(\mathbf{k_T})\big|_{\lambda=-1} = \begin{pmatrix} \frac{c_W\sqrt{2}(m(1-z)+dz)}{Q(\mathbf{k_T}^2+a_W^2)} & \frac{c_W\sqrt{2}z(-k_x+ik_y)}{Q(\mathbf{k_T}^2+a_W^2)} \\ \frac{c_W\sqrt{2}(z-1)(-k_x+ik_y)}{Q(\mathbf{k_T}^2+a_W^2)} & 0 \end{pmatrix}$$

Axial Part

$$\Psi^{W_A}_{q\bar{q}}(\mathbf{k_T})\big|_{\lambda=0} = \begin{pmatrix} \frac{-c_W(m+d)(k_x+ik_y)}{Q(\mathbf{k_T}^2+a_W^2)} & \frac{c_W(2Q^2z(1-z)+(m+d)((1-z)m+zd)}{Q(\mathbf{k_T}^2+a_W^2)} \\ \frac{-c_W(2Q^2z(1-z)+(m+d)((1-z)m+zd)}{Q(\mathbf{k_T}^2+a_W^2)} & \frac{c_W(m+d)(-k_x+ik_y)}{Q(\mathbf{k_T}^2+a_W^2)} \end{pmatrix}$$

$$\Psi^{W_A}_{q\bar{q}}(\mathbf{k_T})\big|_{\lambda=1} = \begin{pmatrix} 0 & \frac{-c_W\sqrt{2}(z-1)(k_x+ik_y)}{Q(\mathbf{k_T}^2+a_W^2)} \\ \frac{c_W\sqrt{2}z(k_x+ik_y)}{Q(\mathbf{k_T}^2+a_W^2)} & \frac{c_W\sqrt{2}(-m(1-z)+dz)}{Q(\mathbf{k_T}^2+a_W^2)} \end{pmatrix}$$

$$\Psi^{W_A}_{q\bar{q}}(\mathbf{k_T})\big|_{\lambda=-1} = \begin{pmatrix} \frac{-c_W\sqrt{2}(-m(1-z)+dz)}{Q(\mathbf{k_T}^2+a_W^2)} & \frac{-c_W\sqrt{2}z(-k_x+ik_y)}{Q(\mathbf{k_T}^2+a_W^2)} \\ \frac{c_W\sqrt{2}(z-1)(-k_x+ik_y)}{Q(\mathbf{k_T}^2+a_W^2)} & 0 \end{pmatrix}$$

where

$$\begin{aligned} a_W^2 &= Q^2z - Q^2z^2 + m^2 - m^2z + zd^2 \quad , \\ \mathbf{k_T} &= (k_x, k_y) \quad , \\ c_W &= g_W\sqrt{N_c} \quad . \end{aligned}$$

In configuration space

Vector Part

$$\Psi^{W_V}_{q\bar{q}}(\mathbf{r_T})\big|_{\lambda=0} =$$

$$\begin{pmatrix} \frac{ic_W(m-d)e^{i\phi}a_W K_1(a_W r_T)}{2\pi Q} & \frac{-ic_W(2Q^2z(1-z)+(m-d)((1-z)m-zd))K_0(a_W r_T)}{2\pi Q} \\ \frac{-ic_W(2Q^2z(1-z)+(m-d)((1-z)m-zd))K_0(a_W r_T)}{2\pi Q} & \frac{-ic_W(m-d)e^{-i\phi}a_W K_1(a_W r_T)}{2\pi Q} \end{pmatrix}$$

$$\Psi^{W_V}_{q\bar{q}}(\mathbf{r_T})\big|_{\lambda=1} = \begin{pmatrix} 0 & \frac{ic_W\sqrt{2}(z-1)e^{i\phi}a_W K_1(a_W r_T)}{2\pi} \\ \frac{ic_W\sqrt{2}ze^{i\phi}a_W K_1(a_W r_T)}{2\pi} & \frac{ic_W\sqrt{2}(m(1-z)+dz)K_0(a_W r_T)}{2\pi} \end{pmatrix}$$

$$\Psi^{W_V}_{q\bar{q}}(\mathbf{r_T})\big|_{\lambda=-1} = \begin{pmatrix} \frac{ic_W\sqrt{2}(m(1-z)+dz)K_0(a_W r_T)}{2\pi} & \frac{-ic_W\sqrt{2}ze^{-i\phi}a_W K_1(a_W r_T)}{2\pi} \\ \frac{-ic_W\sqrt{2}(z-1)e^{-i\phi}a_W K_1(a_W r_T)}{2\pi} & 0 \end{pmatrix}$$

Axial Part

$$\Psi^{W_A}_{q\bar{q}}(\mathbf{r_T})\big|_{\lambda=0} =$$

$$\begin{pmatrix} \frac{ic_W(m+d)e^{i\phi}a_W K_1(a_W r_T)}{2\pi Q} & \frac{ic_W(2Q^2z(1-z)+(m+d)((1-z)m+zd))K_0(a_W r_T)}{2\pi Q} \\ \frac{-ic_W(2Q^2z(1-z)+(m+d)((1-z)m+zd))K_0(a_W r_T)}{2\pi Q} & \frac{ic_W(m+d)e^{-i\phi}a_W K_1(a_W r_T)}{2\pi Q} \end{pmatrix}$$

$$\Psi^{W_A}_{q\bar{q}}(\mathbf{r_T})\big|_{\lambda=1} = \begin{pmatrix} 0 & \frac{-ic_W\sqrt{2}(z-1)e^{i\phi}a_W K_1(a_W r_T)}{2\pi} \\ \frac{ic_W\sqrt{2}ze^{i\phi}a_W K_1(a_W r_T)}{2\pi} & \frac{-ic_W\sqrt{2}(m(1-z)-dz)K_0(a_W r_T)}{2\pi} \end{pmatrix}$$

$$\Psi^{W_A}_{q\bar{q}}(\mathbf{r_T})\big|_{\lambda=-1} = \begin{pmatrix} \frac{ic_W\sqrt{2}(m(1-z)-dz)K_0(a_W r_T)}{2\pi} & \frac{ic_W\sqrt{2}ze^{-i\phi}a_W K_1(a_W r_T)}{2\pi} \\ \frac{-ic_W\sqrt{2}(z-1)e^{-i\phi}a_W K_1(a_W r_T)}{2\pi} & 0 \end{pmatrix}$$

where

$$\begin{aligned} a_W^2 &= Q^2z - Q^2z^2 + m^2 - m^2z + zd^2 \quad , \\ \mathbf{k_T} &= (k_x, k_y) \quad , \\ c_W &= g_W\sqrt{N_c} \quad . \end{aligned}$$

4.2.2 Pion Wave Function

We write explicitly only the wave functions in configuration space, since by now the reader should be able to easily switch from configuration space to momentum space taking the Fourier transform, using as an example the expressions for the W boson WF. From 3.20 we get

$$\Psi^{\pi}_{q\bar{q}}(\mathbf{r_T}) = \begin{pmatrix} \frac{ic_\pi e^{i\phi} a_\pi K_1(a_\pi r_T)}{2\pi} & \frac{c_\pi(m-zm+dz)K_0(a_\pi r_T)}{2\pi} \\ \frac{-c_\pi(m-zm+dz)K_0(a_\pi r_T)}{2\pi} & \frac{ic_\pi e^{-i\phi} a_\pi K_1(a_\pi r_T)}{2\pi} \end{pmatrix}.$$

where

$$a_\pi^2 = -m^2 z + m^2 + zd^2 + m_\pi^2 z^2 - m_\pi^2 z\,,$$
$$c_\pi = \frac{M}{f_\pi}\,.$$

M is the constituent quark mass. We take $\frac{M}{f_\pi} \approx 2$ ([15]).

4.3 Vanishing contributions: vector and transverse axial currents

It is reasonable to think that the vector part of the weak current cannot produce scalar pions, because a vector virtual particle cannot produce diffractively a scalar particle (the pion) at least in the BD limit, since it does not have in its light cone expansion any scalar terms. Then, its contribution to the hadronic current (i.e., to the coefficients c_L and $c_{\pm 1}$) should vanish. Let's separate the vector and axial parts of each coefficient as follows, with an obvious notation,

$$c_L = c_L^v + c_L^a\,,$$
$$c_{\pm 1} = c_{\pm 1}^v + c_{\pm 1}^a\,.$$

In order to prove that $c_{\pm 1}^v = 0$ and $c_L^v = 0$, we have to calculate the hadronic current given in 3.27. For this purpose, it is easier to first multiply the pion and W boson wave functions for the different values of λ, then to sum over helicities, and finally to integrate starting with the azimuthal integral over ϕ. Following these instructions, we see that for $\lambda = 0$ with the pion WF given by 3.20 and the vector part of the W boson WF given in 4.2.1, we obtain immediately $c_L^v = 0$ after multiplying the WF and summing over helicities. For $\lambda = \pm 1$ we obtain after summing over helicities a non-vanishing result, but this result is proportional to $e^{i\phi}$, so after integrating over the azimuthal angle it vanishes. Then we obtain $c_1^v = 0$ and $c_{-1}^v = 0$. We conclude that the vector current gives no contribution to the process for this pion WF, not only in the BD limit, but also in the case where we use a phenomenological scattering amplitude.

On the other hand, the axial part of the W boson wave function does contribute to the process. However, following a very similar analysis we see that $c_{\pm 1}^a$ also vanishes, so that $c_{\pm 1} = 0$. Then, the only relevant coefficient is $c_L = c_L^a$, so in the following sections we will concentrate in studying the longitudinal axial part of the current and its non vanishing contributions to the process.

4.4 Simplest model: black disc limit

In the black disc limit, the scattering amplitude $\mathcal{A}$ has to be replaced by a constant. In this case, we have

$$c_L \propto \sum_{\lambda_1,\lambda_2} \int d^2\mathbf{r_T} dz \Psi_\pi^*(\mathbf{r_T}, z, m_\pi^2, q'_+, \lambda_1, \lambda_2) \Psi_{W_A}(\mathbf{r_T}, z, Q^2, q_+, \lambda_1, \lambda_2, \lambda = 0)\,. \quad (4.2)$$

After multiplying the WF given in 4.2.1 and summing over helicities we obtain

$$c_L = \frac{c_\pi c_W}{\pi Q} \int d^2\mathbf{r_T} dz (\alpha K_1(a_\pi r_T) K_1(a_W r_T) + \beta K_0(a_\pi r_T) K_0(a_W r_T)) \,, \tag{4.3}$$

where

$$\begin{aligned} \alpha &= -a_\pi a_W (m+d) \\ \beta &= -dm^2 - m^3 + 2m^3 z - 2md^2 z - mQ^2 z + 4mQ^2 z^2 - m^3 z^2 \qquad (4.4) \\ &\quad + md^2 z^2 - 2mQ^2 z^3 + dm^2 z^2 - d^3 z^2 - 2dQ^2 z^2 + 2dQ^2 z^3 \,. \qquad (4.5) \end{aligned}$$

The first important observation is that the integral diverges, because both the pion and W boson WF have terms proportional to $K_1(r_T)$ in configuration space.

The second observation is that the results are proportional to the quark masses. This does not mean that in the chiral limit these results vanish, because the quark masses that need to be used here are not the physical quark masses, but phenomenological quantities that play the role of infrared cutoffs, of the order of Λ_{QCD} ([6]).

Third, h^μ has non vanishing terms proportional to the longitudinal polarization vector ε_L. This is interesting because from the meson model in the BD limit, we were expecting only terms proportional to q^μ, which give a vanishing contribution to the process due to lepton current conservation. Then, our first conclusion is that the meson model and the color dipole model are not equivalent in the BD limit, at least if perturbative wave functions for the W boson and pion are used.

These results *have to be interpreted with care*, because the model gives a *divergent scattering amplitude* due to the absence of color transparency (CT removes the small r_T divergences in the wave functions), so in order to obtain a reasonable approximation, we have to proceed to our second model, which takes into account color transparency.

4.5 Second model: phenomenological dipole cross section

To make the model more realistic, we have to introduce a phenomenological dipole cross section. We will use the energy-dependent parametrization of [16] and [17] , given by

$$\sigma^p_{q\bar{q}}(\mathbf{r_T}) = \sigma_0(s'_n) \left(1 - \exp\left(-\frac{\mathbf{r_T}^2}{r_0^2(s'_n)}\right)\right) \,, \tag{4.6}$$

where

$$\sigma_0(s) = \sigma^{\pi p}(s'_n) \left(1 + \frac{3r_0^2(s')}{8 < r_{ch}^2 >}\right), \qquad \sigma^{\pi p}(s'_n) = \Sigma_0 + \Sigma_1 \ln^2(s'_n/s_0) \,. \tag{4.7}$$

and s'_n is the CM energy squared of the W boson-nucleon system. The parameters used in 4.6 and 4.7 are given in table 4.5.

On the other hand, the nucleus profile function $T(b)$ can be obtained using [1]

$$T(\mathbf{b}) = \int_{-\infty}^{\infty} \rho(b, z') dz' \,, \tag{4.8}$$

where the nuclear density ρ is given by the Woods-Saxon parametrization,

$$\rho(r) = \frac{\rho_0}{(1 + \exp((r-R)/a))} \,, \tag{4.9}$$

and

$$\rho_0 = \frac{3A}{4\pi R^3} \frac{1}{1 + \pi^2 a^2 / R^2} \,. \tag{4.10}$$

The parameters A, R and a are tabulated in [1]. We will use $A = 207$, $R = 6.62[fm]$, and $a = 0.546[fm]$.

Σ_0	$20.9[mb]$
Σ_1	$0.31[mb]$
s_0	$28.9[GeV^2]$
s_1	$1000[GeV^2]$
$r_0(s'_n)$	$0.88\left(\frac{s'_n}{s_1}\right)^{0.14}[fm]$
$< r^2_{ch} >$	$0.44[fm^2]$

Table 1: Dipole CS parameters

4.5.1 Some comments on the numerical calculations

In the following sections we will need to calculate c_L for different values of ν, Q^2 and t. The major problem with these calculations is that the scattering amplitude of the dipole is a sum with as many terms as the number of nucleons in the nucleus (see eq. 6.45), that in our case is quite big, and that after summing, a two dimensional integral has to be carried out for each value of Q^2, ν and t.

To speed up the calculations, we used the fact that only the first terms in the aforementioned sum contribute to the results, and the higher order terms are negligible. For this reason, we only take the first 25-30 terms in the sum 6.45, that ensure that the error in the calculation of the amplitude is smaller than $1 \cdot 10^{-6}$ at large r_T. With this simplification, in section 4.5.3 we integrate over r_T and z to obtain c_L for a mesh of $40x60x30$ points in the $Q^2 - \nu - t$ plane. After integrating, we make an interpolation to obtain a mesh of $100x100x300$ points, to be able to integrate over Q^2, ν and t using the mid-point rule with accuracy. The results for section 4.5.2 are obtained by following a similar methodology.

All the calculations were done using Maple, and they are analytical until we are forced to use numerical methods to integrate over r_T and z to obtain c_L. A precision of 4 digits is used in the integration routines. A CD copy of the main Maple worksheets is included in the back cover of this work.

4.5.2 Diffractive production of pions by longitudinal W bosons

It is important to analyze this cross section, because it will show that the coefficient c_L is different from zero and gives a non vanishing cross section for diffractive production of pions by longitudinal W bosons, contradicting the results given by the meson dominance model in the BD limit. Using 2.9, 2.10 and 3.27, we obtain for a longitudinally polarized W boson

$$\mathcal{M}_h = c_L \,. \tag{4.11}$$

Then, using 2.12 and 4.1 we have

$$\frac{d\sigma}{dt} = \frac{1}{16\pi\lambda(s', q^2, m_N^2)} |c_L|^2 \,. \tag{4.12}$$

There is one kinematical detail that has to be taken into account. In the W boson-nucleus CM system where the momenta of the initial particles lie on the z axis, the transferred momentum squared is

$$t = -Q^2 + m_\pi^2 - 2q_0 q'_0 + 2q_z q'_z \cos(\theta) \,, \tag{4.13}$$

where q_0 and q_0' are the energies of the virtual W boson and final pion respectively, and q_z and q_z' their momentum. They are given in therms of the total CM energy squared, s' by

$$\begin{aligned} q_0 &= \frac{s' - Q^2 - m_N^2}{2\sqrt{s'}}\,, \\ q_0' &= \frac{s' + m_\pi^2 - m_N^2}{2\sqrt{s'}}\,, \\ q_z &= \sqrt{q_0^2 + Q^2}\,, \\ q_z' &= \sqrt{q_0'^2 - m_\pi^2}\,. \end{aligned} \tag{4.14}$$

It is not hard to see that t is always negative. But it is important to notice that $|t|$ takes its minimum and maximum values depending on the value of $\cos(\theta)$. These values are given by

$$\max|t| = -Q^2 + m_\pi^2 - 2q_0q_0' + 2q_zq_z'\,, \tag{4.15}$$

$$\min|t| = -Q^2 + m_\pi^2 - 2q_0q_0' - 2q_zq_z'\,. \tag{4.16}$$

Using 4.14 in 4.16 and remembering that $s' = -Q^2 + m_N^2 + 2\nu m_N$ it is possible to find these minimum and maximum values as functions of Q, ν and the masses of the nucleus and the pion. This is important because the kinematical restriction on the minimum value of $|t|$ will prevent the process from happening in some cases, regardless of the phenomenological model used to describe the process. The maximum value of $|t|$ does not matter, because the process is suppressed by the decay of the cross section before reaching this maximum.

We will study two cases, to make clear the aforementioned point. First, we use the values for the kinematical variables given in table 2, and we plot the differential cross section as function of $|t|$ in fig. 4.1.

Q	$3[GeV]$
ν	$10[GeV]$
m_N	$193[GeV]$

Table 2: Values for the parameters

.

We see that the differential cross section is non-vanishing for values of $|t| < 0.01[GeV^2]$, and it rapidly decreases for large $|t|$. However, using 4.14 and 4.16 we see that for these values of Q and ν, $\min(|t|) \approx 0.2[GeV^2]$, so no values of $|t| < 0.2[GeV^2]$ are allowed. But for values of $|t| > 0.2[GeV^2]$, the differential cross section is very small, and therefore the process does not take place for these values of Q and ν.

Then, it is worth analyzing the behavior of $\min|t|$ as a function of Q and ν, to see for which values of Q and ν we could allow the smallest value of $\min|t|$ possible, so that the process could take place (keep in mind that for large $|t|$, the process is suppressed by the decay of the differential cross section). We plot $\min|t|$ as a function of Q^2 for fixed $\nu = 10[GeV]$ and as a function of ν for fixed $Q^2 = 5[GeV^2]$ in figure 4.2 and 4.3 respectively.

We see that for fixed ν, the value of $\min|t|$ increases rapidly with Q^2. For $Q^2 \approx 0, \nu = 10[GeV]$, $\min|t|$ is almost zero (a precise calculation gives $\min|t| = 1 \cdot 10^{-6}[GeV^2]$), but

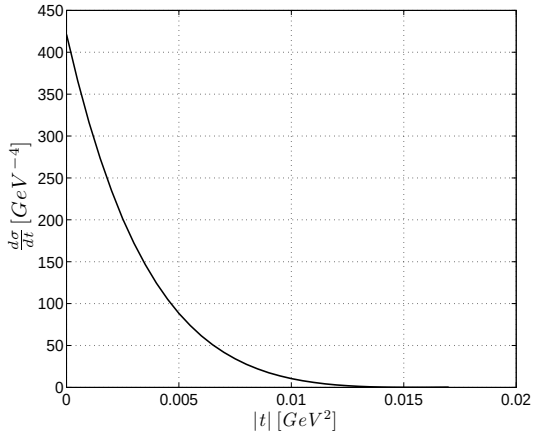

Figure 4.1: **Differential cross section,** $\nu = 10[GeV]$

already for $Q^2 \approx 2[GeV^2]$, $\min|t|$ is close to $0.01[GeV^2]$, which is a value for which the differential cross section already decreased significantly (see 4.1).

On the other hand, for fixed Q^2 we see that $\min|t|$ decreases rapidly for higher energies ν. We see that we need energies $\nu > 25[GeV]$ to allow values of $t < 0.01[GeV^2]$ when $Q^2 = 5[GeV^2]$.

This analysis leads us to the conclusion that in order to allow the production of scalar pions for values of $Q^2 > 5[GeV^2]$, the only alternative is to have values of $\nu > 25[GeV]$. On the other hand, it is possible to produce scalar pions for lower values of ν, only if we study the very small Q^2 regime. Additionally, we have the constrain on Bjorken's variable (for the color dipole model to be valid)

$$x = \frac{Q^2}{2m_n\nu} < \varepsilon\,, \tag{4.17}$$

where $\varepsilon < 0.02$. This constrain also tell us that ν has to be significantly larger than Q^2. Then, depending on how stringent are we with the value of ε, either the constrain on $\min|t|$ or on ϵ will restrict our analysis to the kinematical region of high ν and low Q^2.

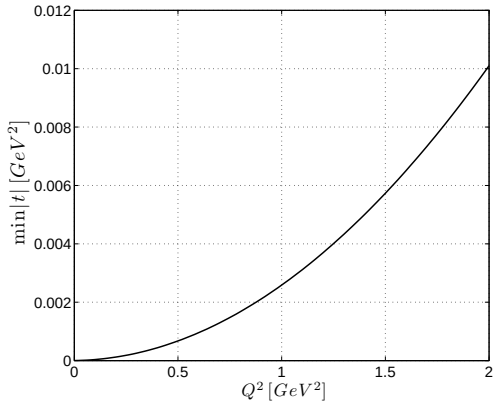

Figure 4.2: $\min|t|$ **for** $\nu = 10[GeV]$

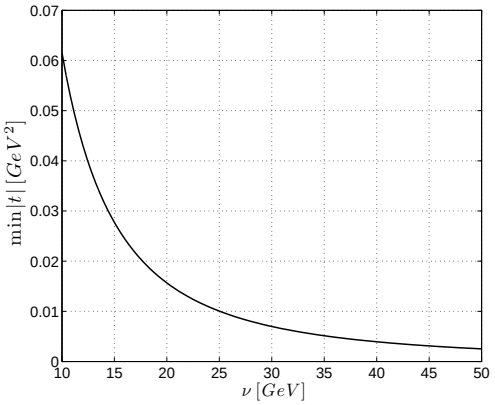

Figure 4.3: $\min|t|$ **for** $Q^2 = 5[GeV^2]$

Now, let's analyze the second case, with the values for the kinematical variables given in 3, where we consider a higher value for ν. For these values, $\min|t| \approx 0.008[GeV^2]$, so the

differential cross section is plotted starting from $|t| = 0.008[GeV^2]$ in figure 4.4. We see that the differential cross section in this case is non vanishing for the allowed values of $|t|$. Integrating, we obtain the total cross sections

$$\int_{\min|t|}^{\infty} dt \frac{d\sigma}{dt} = 14.9[\mu b]\,. \tag{4.18}$$

Q	$3[GeV]$
ν	$50[GeV]$
m_N	$193[GeV]$

Table 3: Values for the parameters

.

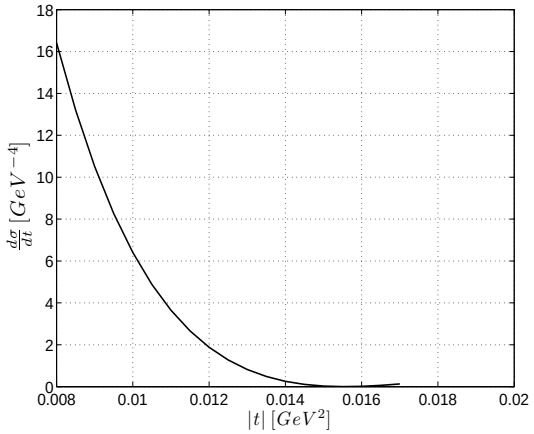

Figure 4.4: **Differential cross section,** $\nu = 50[GeV]$

It is worth mentioning that less than 20% of this cross section comes from the contribution of dipoles with different quark helicities. Finally, we analyze the behavior of the differential cross section as a function of Q^2 and ν, for fixed $t = 9.5 \cdot 10^{-3}[GeV^2]$. This will give us important information about the kinematical region where pion production takes place.

In figure 4.5 we plot the differential cross section as a function of Q^2 for $\nu = 50[GeV]$. We see that it decreases rapidly with Q^2, due to the shape of the wave functions. On the other hand, in figure 4.6 we plot the the differential cross section as a function of ν, for fixed $Q^2 = 1[GeV^2]$. We see that the differential cross section decreases rapidly in the small ν region ($\nu < 20[GeV]$), and that it maintains a moderate decrease with energy for higher values of ν. This dependence on the energy is due to the fact that for higher values of ν, the dipole cross section saturates at higher values of the dipole's transverse separation r_T.

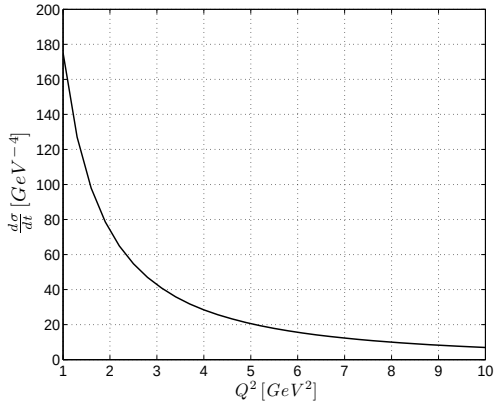

Figure 4.5: **Differential cross section as function of Q^2**

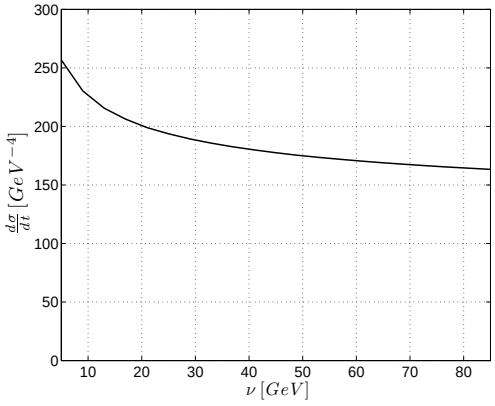

Figure 4.6: **Differential cross section as function of ν**

4.5.3 Pion production by scattering of neutrinos off nuclei: first attempt

Now we turn to the final problem of calculating the cross section for the process 2.1. The Feynman amplitude is given by eq. 2.1, 2.10 and 3.27 by

$$\mathcal{M} = \frac{g_W}{m_W^2}\varepsilon_L^\mu l_\mu c_L\,. \tag{4.19}$$

Taking the amplitude squared and using 2.3 and 2.11, we obtain

$$|\mathcal{M}|^2 = \left(\frac{g_W}{m_W^2}\right)^2 \left(\frac{4E^2 - 4E\nu - Q^2}{\nu^2 + Q^2}\right) \frac{Q^2}{2} |c_L|^2\,, \tag{4.20}$$

so using eq. 2.7 we get

$$\frac{d\sigma}{dQ^2 d\nu dt} = \left(\frac{g_W}{m_W^2}\right)^2 \frac{Q^2}{2}$$
$$\frac{\left(4m_N^2|\mathbf{q}'|^2 - t(t+Q^2-m_\pi^2) - 2\nu m_N(t+m_\pi^2+Q^2)\right)\left(4E^2-4E\nu-Q^2\right)}{96 m_N^2 E^2 |\mathbf{q}'|^2 \lambda(s',q^2,m_N^2)(2\pi)^3\sqrt{\nu^2+Q^2}} |c_L|^2\,. \tag{4.21}$$

We are now ready to analyze the results of the model. We integrate over $|t|$, and we plot the differential cross section $\frac{d\sigma}{dQ^2 d\nu}$ in figure 4.7. The first observation is that the contribution to the total cross section comes mainly from small values of Q^2 and ν. The decrease of the differential cross section with respect to Q^2 is due to the shape of the wave functions (i.e., to the color dipole model itself) and to a less extent, due to the kinematical factors. On the contrary, the decrease with ν is mainly produced by the kinematical factors, and to a less extent, to the color dipole model itself.

To obtain the total cross section, we have to take into account the common assumption that the model is valid only in the region $x = \frac{Q^2}{2m_n\nu} < 0.02$. Then, we integrate only over the region Ω in the $Q^2 - \nu$ plane that fulfills this condition, and we obtain

$$\int_\Omega dQ^2 d\nu \frac{d\sigma}{dQ^2 d\nu} \approx 127[fb]\,. \tag{4.22}$$

A cross section of 127 femto barns is more than ten times the cross section of production of pions given in ([1]) for lighter nuclei, so there is something wrong. There is one important problem in our analysis: the major contributions to the cross section comes from the small $\nu - Q^2$ region. We will discuss this difficulty in the following section.

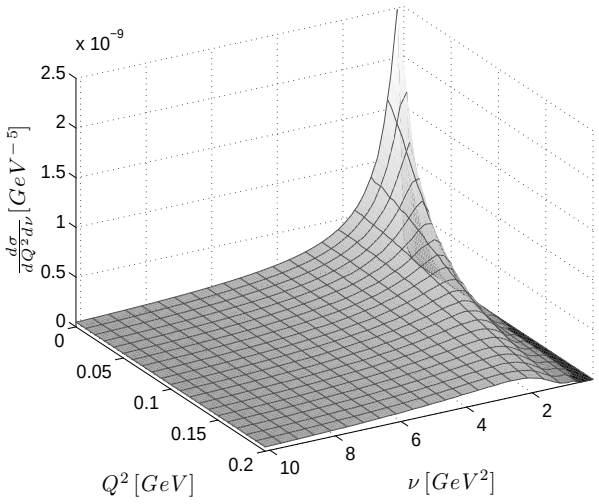

Figure 4.7: **Differential cross section for scalar pion productions, E=20[GeV]**

4.6 Dipole lifetime and Fourier analysis of the dipole model

To make clear that being in the low $\nu - Q^2$ region is in fact a difficulty, we have to study the dipole lifetime. The exact expression for the lifetime of the dipoles is (see app. 6.1)

$$\tau = \frac{1}{\Delta E} = \frac{2q^+}{Q^2 + \frac{\mathbf{k_T}^2 + m^2(1-z) + d^2 z}{z(1-z)}}\,. \tag{4.23}$$

For our big nucleus ($A = 207$), we need $\tau > 50[GeV^{-1}]$. The problem is that for small Q^2, the dipole lifetime near $z = 0$ and $z = 1$ is very small, so these dipoles do not live enough to travel through the nucleus, and the model looses its validity. Additionally, the dipole lifetime is smaller for higher values of $\mathbf{k_T}^2$. A workaround for this problem would be to consider only the dipoles which for fixed Q^2 and ν, have values of $\mathbf{k_T}^2$ and z that allow large dipole lifetimes. This is not really a solution to the problem, because other physical processes which contribute in a different way to the cross section are taking place for those short lived dipoles. However, if we exclude the problematic dipoles from the analysis, we can find a lower bound for the total cross section in the color dipole model. In order to accomplish this task, we have to study the Fourier decomposition of the Feynman amplitude. Recalling eq. 4.1 we have

$$c_L = \sum_{\lambda_1,\lambda_2} \int dz d^2\mathbf{k'_T} d^2\mathbf{r_T} \exp(-i\mathbf{k'_T}\cdot\mathbf{r_T}) \mathcal{F}\Big\{\Psi^*_\pi(\mathbf{r_T})\Psi_W(\mathbf{r_T},\lambda=0)\mathcal{A}(\mathbf{r_T})\Big\}(\mathbf{k'_T})\,, \tag{4.24}$$

where $\mathcal{F}\{f(\mathbf{r_T})\}(\mathbf{k'_T})$ denotes the fourier transform of the function $f(\mathbf{r_T})$, as a function of $\mathbf{k'_T}$. Integrating over $\mathbf{r_T}$ and $\mathbf{k'_T}$ the expression reduces to

$$c_L = \sum_{\lambda_1,\lambda_2} \int dz \mathcal{F}\Big\{\Psi^*_\pi(\mathbf{r_T})\Psi_W(\mathbf{r_T},\lambda=0)\mathcal{A}(\mathbf{r_T})\Big\}(0)\,, \tag{4.25}$$

and using the convolution property of the Fourier transform we obtain

$$c_L = \sum_{\lambda_1,\lambda_2} \int dz d^2\mathbf{k_T} \mathcal{F}\Big\{\Psi^*_\pi(\mathbf{r_T})\mathcal{A}(\mathbf{r_T})\Big\}(-\mathbf{k_T})\Psi_W(\mathbf{k_T},\lambda=0)\,, \tag{4.26}$$

where we already know the function $\Psi_W(\mathbf{k_T},\lambda=0)$ from section 4.2.1. This expression allows us to study the contribution of each momentum $\mathbf{k_T}$ to the process. In principle, an

exact analysis could be carried out by integrating only over the values of z and $\mathbf{k_T}$ which give $\tau > 50[GeV^{-1}]$ for each value of ν and Q^2. However, this method would be very hard to implement numerically, since instead of the three dimensional integral needed to calculate c_L in transverse separation space, a five dimensional integral is needed in transverse momentum space. Instead of that, we can analyze the Fourier decomposition of c_L, and see which are the typical values of $\mathbf{k_T} = \overline{\mathbf{k}}_\mathbf{T}(\nu, Q^2, t, z)$ that contribute to the process, and calculate c_L in configuration space, over the values of z which satisfy the condition

$$\tau = \frac{2q^+}{Q^2 + \frac{\overline{\mathbf{k}}_\mathbf{T}^2 + m^2(1-z) + d^2 z}{z(1-z)}} > 50[GeV^{-1}]\,. \tag{4.27}$$

Even the task of finding $\overline{\mathbf{k}}_\mathbf{T}$ can be computationally intensive, but fortunately we can solve part of the integrals analytically. Let's start by studying the contribution of the dipoles with equal helicities, $\lambda_1 = \lambda_2$. Recalling the pion WF of section 4.2.1, we have

$$\begin{aligned}\mathcal{F}\Big\{\Psi_\pi^*(\mathbf{r_T}, \lambda_\mathbf{1} = \lambda_\mathbf{2})\mathcal{A}(\mathbf{r_T})\Big\}(-\mathbf{k_T}) &\propto \mathcal{F}\Big\{\exp(-i\phi)K_1(a_\pi r_T)\mathcal{A}(\mathbf{r_T})\Big\}(-\mathbf{k_T}) \\ &= \int d^2\mathbf{r_T} \exp(-i(\mathbf{k_T}\cdot\mathbf{r_T} + \phi))K_1(a_\pi r_T)\mathcal{A}(\mathbf{r_T})\ ,. \end{aligned} \tag{4.28}$$

Using $\mathbf{k_T}\cdot\mathbf{r_T} = k_T r_T \cos(\theta_k - \phi)$, where θ_k is the angle that $\mathbf{k_T}$ forms with the x axis, we obtain after integrating over the angle of $\mathbf{r_T}$ ($\mathcal{A}(\mathbf{r_T})$ does not depend on the angles, only on r_T),

$$\mathcal{F}\Big\{\Psi_\pi^*(\mathbf{r_T}, \lambda_1 = \lambda_2)\mathcal{A}(\mathbf{r_T})\Big\}(-\mathbf{k_T}) \propto \exp(-i\theta_k)\int dr_T r_T J_1(k_T r_T)K_1(a_\pi r_T)\mathcal{A}(\mathbf{r_T})\,,$$

so that using the W boson wave function we have

$$\begin{aligned} c_L(\lambda_1 = \lambda_2) &\propto \int dz dk_T d\theta_k k_T \Big(\exp(-i\theta_k)\int dr_T r_T J_1(k_T r_T)K_1(a_\pi r_T)\mathcal{A}(\mathbf{r_T})\Big)\frac{k_T\exp(-i\theta_k)}{k_T^2 + a_W^2} \\ &= 2\pi\int dz dk_T \frac{k_T^2}{k_T^2 + a_W^2}\int dr_T r_T J_1(k_T r_T)K_1(a_\pi r_T)\mathcal{A}(\mathbf{r_T})\,. \end{aligned} \tag{4.29}$$

In a similar manner, it is easy to show that

$$\begin{aligned} c_L(\lambda_1 = -\lambda_2) \quad \propto \quad & 2\pi\int dz dk_T (2Q^2 z(1-z) + (m+d)((1-z)m + zd)(m(1-z) + dz) \\ & \frac{k_T}{k_T^2 + a_W^2}\int dr_T r_T J_0(k_T r_T)K_0(a_\pi r_T)\mathcal{A}(\mathbf{r_T})\,. \end{aligned} \tag{4.30}$$

We see from 4.29 and 4.30 that the typical values of $\mathbf{k_T}$ are controlled by the functions

$$\xi_1 = \frac{k_T^2}{k_T^2 + a_W^2}\int dr_T r_T J_1(k_T r_T)K_1(a_\pi r_T)\mathcal{A}(\mathbf{r_T})\,, \tag{4.31}$$

$$\xi_2 = \frac{k_T}{k_T^2 + a_W^2}\int dr_T r_T J_0(k_T r_T)K_0(a_\pi r_T)\mathcal{A}(\mathbf{r_T})\,. \tag{4.32}$$

The behavior of ξ_1 and ξ_2 as functions of k_T is plotted in figures 4.8 and 4.9, for $z = 0.8$. We see that the dipoles with equal helicities have typical values of k_T of the order of $0.4[GeV]$, while the dipoles with opposite helicities have smaller values of $\overline{k}_T$, of the order of $0.2[GeV]$. Then we have to concentrate on ξ_1, not only because it peaks at higher values of k_T (smaller dipole lifetimes), but also because the dipoles with equal helicities

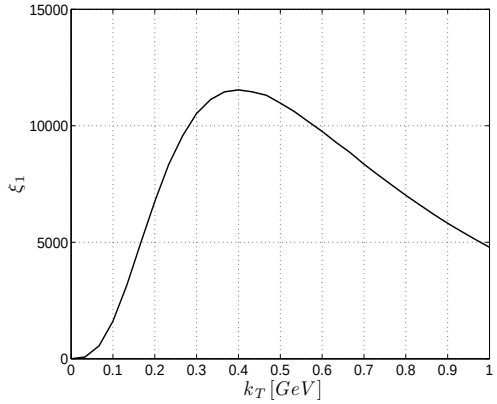

Figure 4.8: $\nu = 10[GeV]$, $Q^2 = 0.1[GeV^2]$, $t = 0.01[GeV^2]$, $z = 0.8$

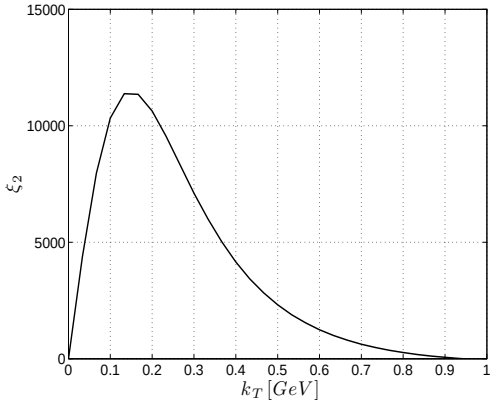

Figure 4.9: $\nu = 10[GeV]$, $Q^2 = 0.1[GeV^2]$, $t = 0.01[GeV^2]$, $z = 0.8$

contribute with more than 80% of the final cross section. From now on, we will use for $\overline{k}_T$, the position of the maximum of the curve $\xi_1(k_T)$.

In principle, $\overline{k}_T$ depends on ν, Q^2 and t. We plot in figures 4.10, 4.11, 4.12 and 4.13 the function $\xi_1(k_T)$ for different values of ν, Q^2, t and z. Note that to improve figure 4.12, we plot $|\xi_1|$ instead of ξ_1, and we normalize it to its maximum, because the function changes sign and because for different values of t, it differs by several orders of magnitude. From these figures, we see that $\overline{k}_T$ does not depend on the variation of ν. There is a slight variation of $\overline{k}_T$ of less than $0.1[GeV^2]$ for different values of Q^2 and t, and a more important variation for different values of z, of the order of $0.2[GeV^2]$. Then, to retain simplicity, we will use $\overline{k}_T(\nu, Q^2, t, z) = \overline{k}_T(z)$.

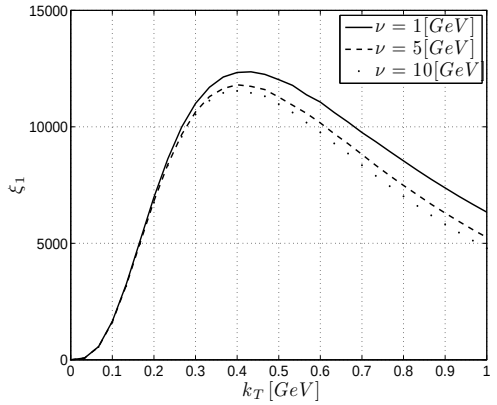

Figure 4.10: $Q^2 = 0.1[GeV^2]$, $t = 0.01[GeV^2]$, $z = 0.8$

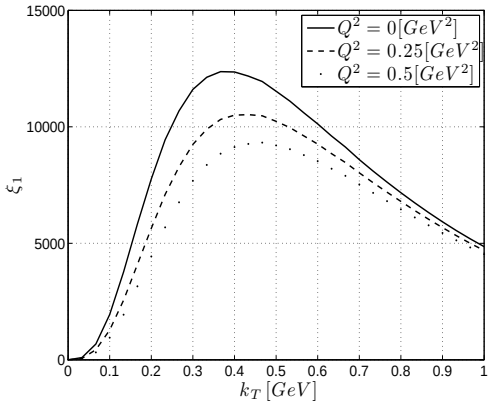

Figure 4.11: $\nu = 10[GeV]$, $t = 0.01[GeV^2]$, $z = 0.8$

In figure 4.14 we plot $\overline{k}_T$ as a function of z. We also plot

$$1.7a_\pi = 1.7\sqrt{-m^2z + m^2 + zd^2 + m_\pi^2 z^2 - m_\pi^2 z}\,,$$

since it provides a good fit for $\overline{k}_T$. This makes sense, because it is reasonable to expect that a_π and a_W (see sec. 4.2.1) are the variables that control the bandwidth of the wave functions.

Finally, we are in the position to analyze the dipole lifetime 4.30, using $\overline{k}_T \approx 1.7a_\pi$. We plot this lifetime in figures 4.15 and 4.16 for different values of ν and Q^2. We see that

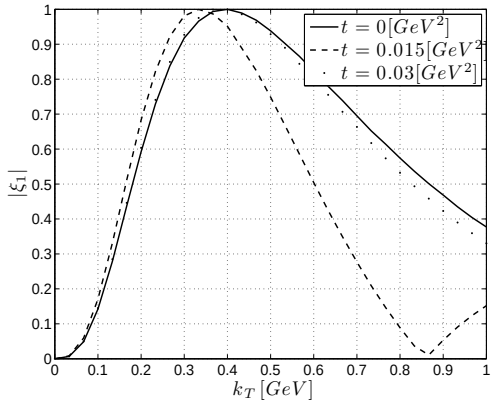

Figure 4.12: $\nu = 10[GeV]$, $Q^2 = 0.1[GeV^2]$, $z = 0.8$

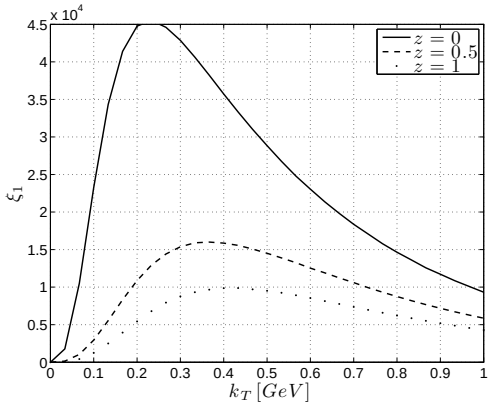

Figure 4.13: $\nu = 10[GeV]$, $Q^2 = 0.1[GeV^2]$,$t = 0.01[GeV^2]$

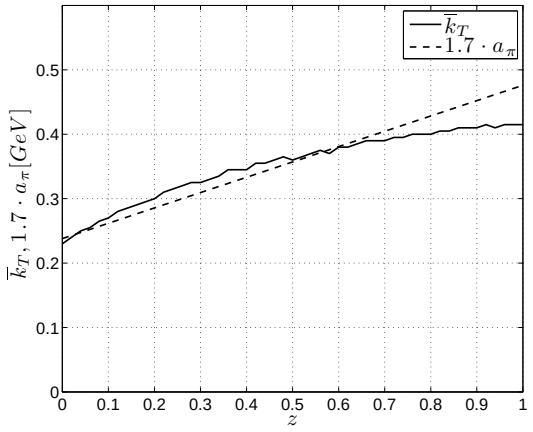

Figure 4.14: **Fit of $\overline{k}_T$ by a_π**, $Q^2 = 0.1[GeV^2]$, $\nu = 10[GeV]$, $t = 0.01[GeV^2]$

as expected, the dipole lifetime increases for higher values of ν, and decreases for higher values of Q^2. In any case, it tends to zero in the limits $z = 0$ and $z = 1$. For some values of ν and Q^2, there is a region $z = [a, b]$ where $\tau > 50[GeV^2]$. For the remaining values of ν and Q^2, $\tau < 50[GeV]$ for every value of z, so these regions are forbidden and have to be removed from the calculation of the total cross section. In the next section we present the results for the cross section using our new constrain for τ.

4.6.1 Pion production by scattering of neutrinos off nuclei: second attempt

We are now in a position where we can calculate again the cross section, with our new constrain for τ,

$$\tau = \frac{2q^+}{Q^2 + \frac{(1.7a_\pi)^2 + m^2(1-z) + d^2 z}{z(1-z)}} > 50[GeV^{-1}]\,. \tag{4.33}$$

For each value of Q^2 and ν we obtain the lower and upper limits of z, a and b, and

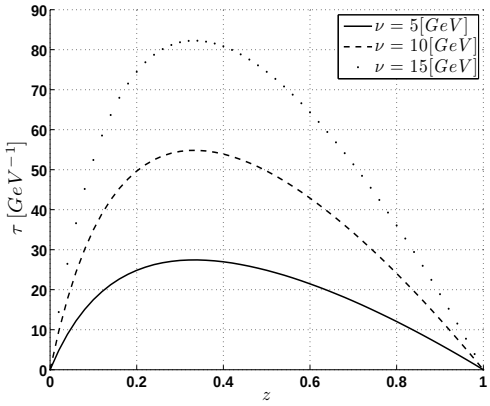

Figure 4.15: **Dipole lifetime for fixed** $Q^2 = 0.1[GeV^2]$

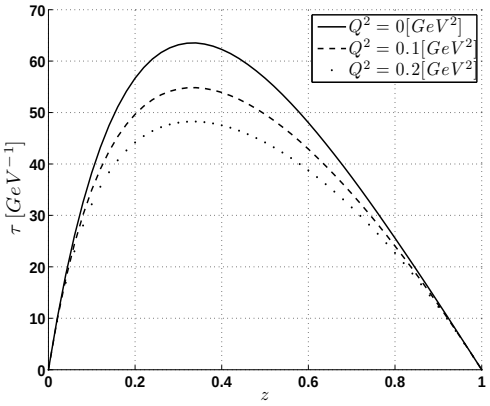

Figure 4.16: **Dipole lifetime for fixed** $\nu = 10[GeV]$

calculate the differential cross section 2.7 using

$$c_L^C = \frac{1}{2}\sum_{\lambda_1,\lambda_2}\int_0^\infty dr_T r_T \int_a^b dz$$
$$\Psi_\pi^*(\mathbf{r_T}, z, m_\pi^2, q'_+, \lambda_1, \lambda_2)\Psi_W(\mathbf{r_T}, z, Q^2, q_+, \lambda_1, \lambda_2, \lambda = 0)\mathcal{A}(\mathbf{r_T})\,. \tag{4.34}$$

We will also make the numerical computations for the amplitude without the cut on z, to get an idea about how important are the dipoles that we cut out,

$$c_L^{NC} = \frac{1}{2}\sum_{\lambda_1,\lambda_2}\int_0^\infty dr_T r_T \int_0^1 dz$$
$$\Psi_\pi^*(\mathbf{r_T}, z, m_\pi^2, q'_+, \lambda_1, \lambda_2)\Psi_W(\mathbf{r_T}, z, Q^2, q_+, \lambda_1, \lambda_2, \lambda = 0)\mathcal{A}(\mathbf{r_T})\,. \tag{4.35}$$

In figures 4.17 and 4.18 we plot the differential cross sections with and without the cut, $\frac{d\sigma^C}{dQ^2 d\nu}$ and $\frac{d\sigma^{NC}}{dQ^2 d\nu}$. Part of the $Q^2 - \nu$ plane is forbidden, because for some values of ν and Q^2, no value of z gives $\tau \geq 50[GeV^{-1}]$. We see from the figures that clearly the problematic dipoles give a large contribution to the cross section. However, even excluding them, we can integrate the differential cross section and we get

$$\int_\Omega dQ^2 d\nu \frac{d\sigma^C}{dQ^2 d\nu} \approx 17.5[fb]\,, \tag{4.36}$$

so that the real total cross section has to be at least of the order of $11[fb]$. If we calculate the cross section without the cut on z, we obtain a result that is more than three times larger (58[fb]).

Another interesting fact of the analysis, is that in figures 4.17 and 4.18 we see that at high energies, the difference between both cross sections decreases, in part because of the kinematical factors, but also because at higher ν, $c_L^{NC} \approx c_L^C$, as the interval limits a and b tend to zero and one, respectively. To note this clearly, we plot c_L^C and c_L^{NC} multiplied by Q (to avoid the singularity at $Q^2 = 0$ that the kinematical factors cancel) for two values of Q^2, as a function of ν and for fixed $t = 0.005[GeV^2]$, in figures 4.19 and 4.20. We see that in any case, for values of $\nu < 15[GeV]$ the two ways of calculating c_L differ significantly. For higher values of ν, the difference is smaller, and for $\nu \approx 30[GeV]$ the difference is smaller than 25%. This means that at higher energies the problems around $z = 0$ and $z = 1$ are less important.

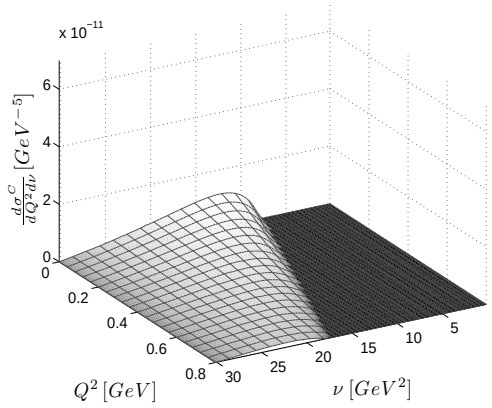

Figure 4.17: **Differential cross section, integral over** $z \in [a,b]$**,**$E = 30[GeV]$

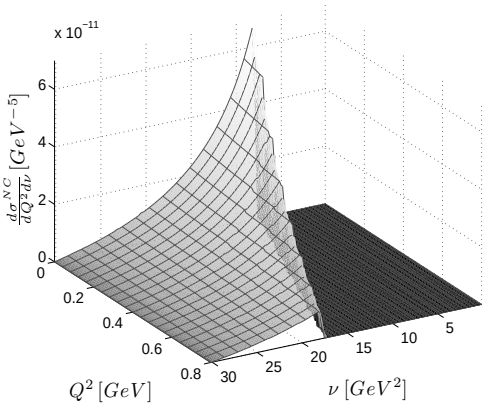

Figure 4.18: **Differential cross section, integral over** $z \in [0,1]$**,** $E = 30[GeV]$

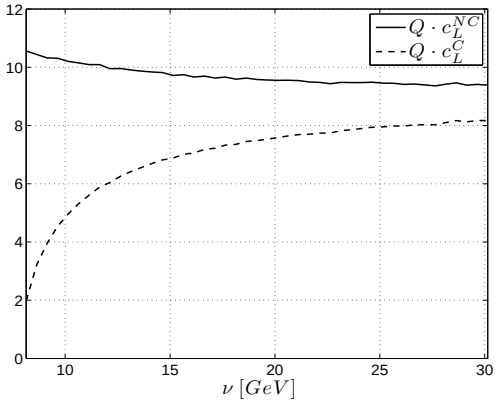

Figure 4.19: **Differential cross section, integral over** $z \in [0,1]$**,**$E = 30[GeV]$**,**$Q^2 = 0[GeV^2]$

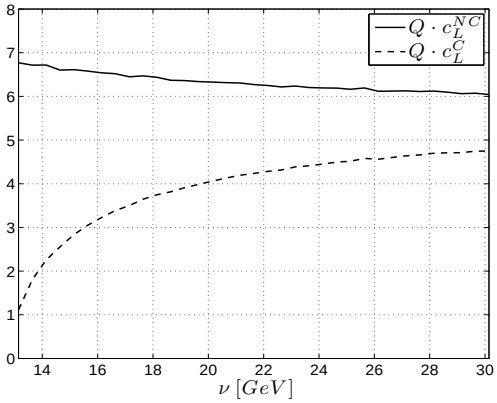

Figure 4.20: **Differential cross section, integral over** $z \in [a,b]$**,** $E = 30[GeV]$**,**$Q^2 = 0.4[GeV^2]$

In figures 4.21 and 4.22 we plot the differential cross section as a function of ν and Q^2. We see that the differential cross section vanishes at small energies because in that region, many dipoles are short-lived so they were excluded from the analysis. The differential cross section as a function of ν grows to its maximum at $\nu \approx 17[GeV]$, where it starts decreasing because of the behavior of the scattering amplitude and kinematical factors. On the other hand, the differential cross section as a function of Q^2 decreases with increasing Q^2, because at higher Q^2 there are less dipoles with large lifetimes and because the wave functions have a decreasing dependence on this variable.

Using c_L^C in figure 4.23 and 4.24 we plot the total cross section as a function of the energy of the incident neutrino and its derivative. We see that the cross section increases with energy, and that there is an inflection point around $E = 60[GeV]$. This increase is due to the fact that for higher energies, the total cross section has to be integrated in ν in a larger interval of energies, and because of the behavior of the kinematical factors.

Finally, to estimate the uncertainty of the model coming from the dipole cross section we use a second model similar to the one presented in 4.6, 4.7 and in table 4.5, but with

$$\sigma^{\pi p}(s'_n) = \left(23.6 \cdot 10^{-3} \left(\frac{s'_n}{s_1}\right)^{0.08}\right)[mb]\,, \tag{4.37}$$

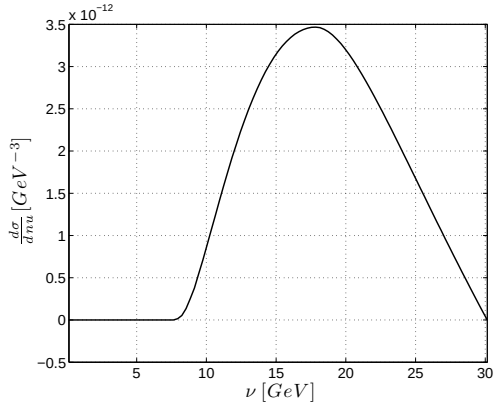

Figure 4.21: **Differential cross section $\frac{d\sigma}{d\nu}$, $E = 30[GeV]$**

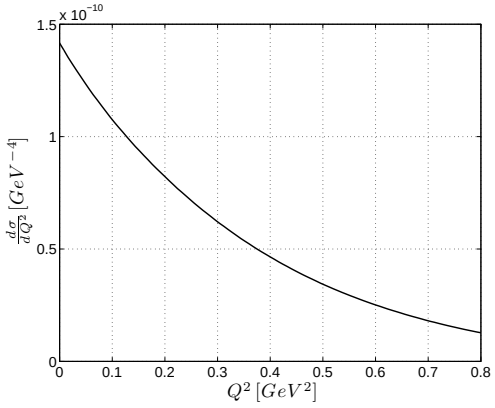

Figure 4.22: **Differential cross section $\frac{d\sigma}{dQ^2}$, $E = 30[GeV]$**

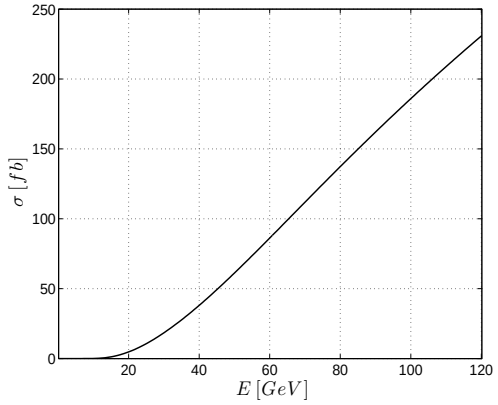

Figure 4.23: **Total cross section as a function of energy**

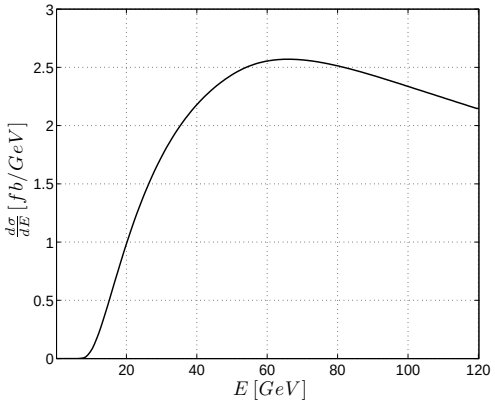

Figure 4.24: **Derivative of the total cross section as a function of energy**

and

$$r_0(s'_n) = 0.88\left(\frac{s'_n}{s_1}\right)^{-0.14}[fm] \tag{4.38}$$

This model is given in reference [16], and it has the advantage that in the limit $s'_n = 0$, the dipole cross section vanishes. This is a good feature, because the shadowing terms coming form Glauber's approach depend on powers of the dipole cross section (see the appendix) and it is known that as the energy ν decreases, the shadowing terms should also vanish. Then, it is good to have a dipole cross section that vanishes at small energies, to supress the shadowing terms.

The results are plotted in figure 4.25 and 4.26. We see that there is an important difference in magnitude with respect to the results given in 4.23, but the shape of the solution is the same, and the inflection point is in the same energy region. Also, the conclusions of this work regarding the problems with the short lived dipoles are the same for both models. It is anyway interesting to show that there is some model uncertainty in the final absolute value of the results. It is also important to mention that another source of uncertainty are the perturbative wave functions. In future analysis, it would be also interesting to try different W boson and pion wave functions, and estimate the variation in the final results.

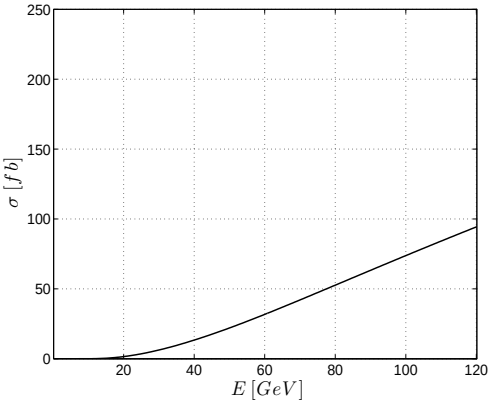

Figure 4.25: **Total cross section as a function of energy**

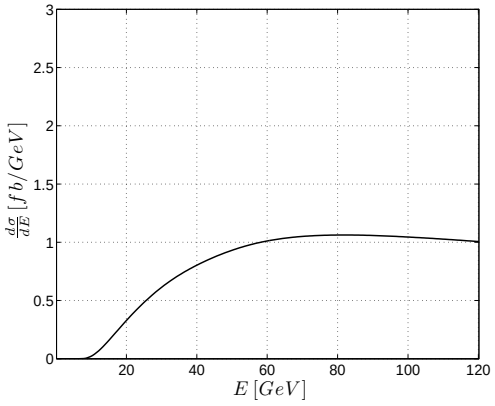

Figure 4.26: **Derivative of the total cross section as a function of energy**

4.7 Comparison with experiments

There is no data for pion production by scattering of neutrinos off heavy nuclei as lead. However, there is data for scattering on lighter nuclei, as Neon. In figure 4.27 we plot the total cross section of pion production by scattering of neutrinos off Neon, mediated by exchange of W bosons. The data is taken from bubble chamber experiments carried out during the eighties [18]. We use the dipole cross section of 4.7. The solid line shows the prediction of the model when we cut the dipoles, and it clearly underestimates the total measured cross section. To obtain this solid curve, we used the restriction that the dipole lifetime should be larger than $20[GeV]$.

The dotted line shows the results when we don't cut the short lived dipoles and surprisingly, this prediction coincides with the experimental results. However, this theoretical prediction is wrong, since the requisites of the model itself are violated. Probably it is only a coincidence that the model with the problematic dipoles fits the data. We know that the short-lived dipoles give a contribution to the total cross section, but calculating this contribution in the frozen dipole approximation should be wrong. If it is not wrong, a different explanation should be given that allow us to also consider the short lived dipoles as frozen.

It is interesting to note that to add the contribution of the short lived dipoles can give confusing results. If we had not done the calculations separately, with and without the cuts, we would have thought that the model is working. For this reason, the problematic dipoles should be always taken into consideration and much care is needed, not only in the frozen dipole model, but also in more sophisticated models that also put constrains on the values of the light cone fraction z, as the Green function approach (see the conclusions).

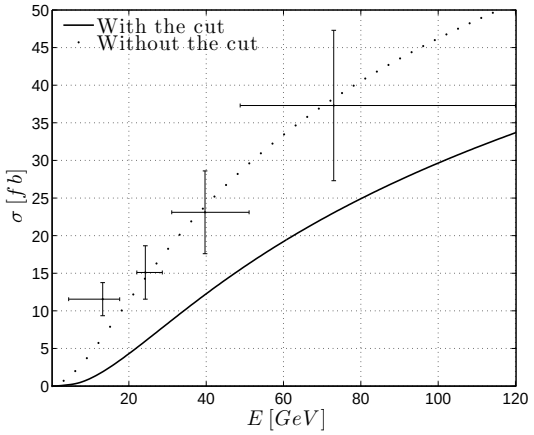

Figure 4.27: **Total coherent pion cross section by scattering of neutrinos off Neon as a function of energy.**

5 Conclusions

The initial motivation of this work was to analyze the black disc limit, by using the color dipole model on heavy nuclei, which are the ideal targets to be treated as black discs. The tempting fact about the black disc limit, is that it provides a very simple model that gives us many (wrong) results without much work. Using the black disc limit, we can easily draw conclusions about processes, only by checking if the initial states are orthogonal to the final ones.

The problem with the BD model is that it easily leads to wrong results, for two reasons. The first one, is that it is too qualitative: it doesn't tell us how heavy has to be the nucleus to behave as a black disc. Here we showed that even in the case of lead, the perfect candidate for a nucleus that could behave as a black disc, the BD model gives wrong results. The second, is that it is non-physical, because it doesn't account for color transparency, so that it gives divergent results because of the small r_T divergences in the wave functions. Surely a cutoff at small transverse separations could be introduced to avoid the small r_T divergences, but then the perfect black disc is lost, alongside with the ability to make predictions by analyzing the orthogonality properties of the initial and final states. In any case, the model seems to be too tricky to be of any use.

Contradicting the results of the BD model, the color dipole model used with a phenomenological dipole cross section, although problematic at low energies, provides a non vanishing cross section for scalar pion production by scattering of neutrinos off heavy nuclei, without requiring much more input than the phenomenological dipole cross section. What is more important is that even in the BD limit, it gives contributions proportional not only to q^μ, but also to the longitudinal polarization vector of the W boson, *contradicting the meson model*. This requires a detailed explanation. The color dipole model gives contributions to the hadronic current that are orthogonal to q^μ (in addition to the ones proportional to q^μ), for a very simple reason: q^μ does not enter in the W boson wave function, because energy-momentum is not conserved in the light front formalism at the W boson - dipole vertex. In turn, the loss of energy momentum conservation has its origin in neglecting the instantaneous propagators of the light front formalism, assumption that is valid only at high energies (see appendix 6.1).

Even if we include again the instantaneous propagators in our perturbative treatment we get contributions orthogonal to q^μ, because then we are allowed to go back to a covariant treatment with integrals over fermion and gluon loops, that in the end give terms proportional to q^μ, but also catch in the loop integrals terms proportional to the final pion momentum ξ^μ and the initial and final nucleus momentum, which have some components that are orthogonal to q^μ.

The meson model gives a different prediction because it assumes that mesons are point-like, and therefore it looses degrees of freedom. Maybe by including multimeson states, these degrees of freedom could be recovered, because only then the quark-gluon description (which includes the dipole state) and the meson description would both form a complete set of states.

Now, the simplicity of the color dipole model breaks down at energies smaller than $20[GeV]$, because for small energies, some (but not all) of the dipoles that we include in the wave functions have very small lifetimes. What is worst, is that these lifetimes are z dependent (z is the light cone momentum fraction, sometimes called α) so that in order to find a mechanism to solve the problem, this mechanism should be able to discern between the "good" and the "bad" values of z. There are treatments that try to solve this problem by interpolating between the dipole-nucleus and the dipole-nucleon cross sections [20], based on the fact that for small dipole lifetimes, the scattering on the nucleus is incoherent (nuclear shadowing disappears) and therefore the dipole-nucleon cross section can be used. However, these mechanisms are at the level of the cross sec-

tion (which was already integrated over z), and not at the level of the integrand of the scattering amplitude (which is z dependent), so that they are "z-blind".

For this reason, it is a bad idea to use $1/x$ at low energies as the quantity that controls the dipole lifetime, and using it despite the warnings that we gave, gives results that are one order of magnitude larger than the ones we can trust. At low energies, the dipole lifetime is z dependent, and it also depends on k_T, the dipole transverse momentum. This is not good, because the dipole model is only simple in transverse separation space and not in transverse momentum space, and dipoles with a fixed transverse separation don't have a definite lifetime. So any exact solution has to be formulated in transverse momentum space using a full Fourier analysis, which is computationally very intensive.

To avoid the full Fourier treatment, we used a reasonable mean value for the lifetime of dipoles with fixed transverse separation, that makes the calculations much easier, and we find the variables that control the Fourier spectra of the dipole model. Using this assumption, we estimate that a lower bound for the pion production cross section is $11[fb]$.

Another possible solution to avoid the problem with the small lifetime of the dipoles is to use the Green's function formalism [21], which takes into account the "fluctuations" of the dipole by modeling its transverse degrees of freedom using a non relativistic harmonic oscillator equation to calculate a Green function, or propagator. The harmonic oscillator potential has both a real part, that takes into account the oscillations of the dipole, and an imaginary part, that accounts for the absorption of some of the dipoles in the nuclear matter. Roughly speaking, the model consists in calculating the scattering amplitude by integrating this Green function over all the paths that the dipole could follow as it travels through the nucleus, to take into account that the transverse size could change with time (or to be more precise, with the longitudinal coordinate). Note that this formalism takes the dipole model very literally, *i.e.*, it considers the dipole to be a "coupled" system that oscillates and that can be absorbed in the nuclear matter. This literal interpretation of the dipole model, although successful in describing data in the intermediate x region, is for the moment still unclear, as there is no definitive approach to give a non perturbative foundation for the dipole model.

Additionally, this formalism has also some troubles. One of the problems is that one should only integrate this Green function over the paths inside the light-cone, that means that one should take into account only the variations in the transverse size of the dipole that occur at a smaller speed than the speed of light. This attempt has not been done. Moreover, the equation for this Green function is non relativistic, and therefore it does not distinguish between paths inside and outside the light cone. What is most disturbing, is that the "mass" of the oscillator is proportional to $\nu(1-z)z$ (note that this is not the invariant mass of the dipole, but the mass of the non relativistic oscillator). Then, if the oscillator is non relativistic, its "energy" (or frequency) must be much smaller than its "mass". However, the frequency Ω divided by the mass $\nu(1-z)z$ is much greater than one for values of z near 0 or 1, so the non relativistic approach also has some problems for these values of z. Maybe the problematic z interval is smaller than the one that we found using the frozen transverse size approximation and Glauber's model, but explicit numerical calculations as the ones done in this work, have to be carried out to see if the problematic values of z or if the paths outside the light cone give a significant contribution to the cross section. If this is the case, our problem is still open, and new alternative solutions have to be investigated.

6 Appendix

6.1 Appendix I: light-cone quantization and the color dipole model

6.1.1 Light cone variables

We use the Lepage-Brodsky convention for light cone four vectors. Any four vector $x^\mu = (x^0, x^1, x^2, x^3)$ written in the light cone form is

$$x^\mu_{LC} = (x^+, x^-, x^1, x^2)\,, \tag{6.1}$$

where $x^+ = x^0 + x^3$, $x^- = x^0 - x^3$. Normally, the subscript LC that we write in order to differentiate LC four vectors from regular four vectors is dropped, so the reader has to be careful and note where regular or LC vectors are being used. We will drop the LC subscript now.

The scalar product of two four vectors can be written as

$$x \cdot p = \frac{1}{2}(x^+p^- + x^-p^+) - \mathbf{x_T} \cdot \mathbf{p_T}\,, \tag{6.2}$$

where $\mathbf{x_T} = (x^1, x^2)$ and $\mathbf{p_T} = (p^1, p^2)$ are called the transverse parts of the four vectors. In particular

$$x^2 = x^+x^- - \mathbf{x_T}^2\,. \tag{6.3}$$

6.1.2 Light cone perturbation theory

The intention of this appendix is not to give a detailed explanation of light cone perturbation theory (LCPT), but just to list the important light cone perturbation rules (LCPR) needed to understand the color dipole model. For this reason, we give a reduced list of the LCPR and a brief introduction to the methodology. A full list and a more detailed explanation of the rules can be found in [10].

LCPT has two main differences with the regular perturbation theory given by the Feynman rules that can be found in most text-books. First, the states are states at a fixed light-cone time x^+ and not at a fixed regular time x^0. Second, the theory is a *time ordered* theory, that means that the Feynman diagrams have a time ordering, which by convention flows from left to right. As a consequence, for each regular Feynman diagram there are many diagrams in LCPT, which correspond to different time orderings of the diagram's vertexes from left to right. Additionally, the number of light cone diagrams are further increased by the fact that there are additional diagrams that correspond to instantaneous propagators (we will discuss these diagrams later).

There are two ways to derive the LCPR. The first one is to quantize the theory at a fixed light cone time. This mechanism is not a new one with respect to the usual quantization found in text books (at fixed regular time), because the canonical commutation relations for an operator are always [22]

$$[\phi(x), \phi(y)] = i\Delta(x - y)\,, \tag{6.4}$$

where Δ is the Feynman function and x, y are arbitrary four vectors. In regular perturbation theory, we use relation 6.4 at $x^0 = y^0$ and in light cone perturbation theory we use the same relation but at $x^+ = y^+$. Then, the difference in both theories does not come from a different quantization prescription, but from the definition of the states: in one theory states are evolved with a hamiltonian in the regular time x^0, and in the other they are evolved in a light cone time x^+. Once one formulates the theory in these terms (see for example [29]) it is possible to obtain the LCPR.

The second way to obtain these rules is by using regular perturbation rules, and integrating in each loop over the minus component of the momenta. This is not a formal procedure, as it has not been proved to be completely analogue to the light cone quantization mechanism, but there are some examples [25] [27] that are successful in reproducing the results of light cone perturbation theory. We will use this mechanism in the following section and relate it to the instantaneous terms to understand the color dipole model.

The light-cone perturbation rules are:

1. Assign a momentum k^μ to each particle line, so that each particle is *on-shell*. The plus and transverse components of the momenta are conserved at each vertex, and the minus component is fixed by the on-shell condition, i.e., $k^- = (\mathbf{k_T^2} + m^2)/k^+$.

2. Include a factor $\theta(k^+)$ for each line, i.e., all particles are forward moving (because to use LCPR is the same as working in the infinite momentum frame).

3. For each vector boson line include a factor $\sum_{\lambda=1,2} \varepsilon_\mu(k,\lambda)\varepsilon_\nu(k,\lambda)/k^+$.

4. The vector boson-fermion vertices are

$$g\frac{\bar{u}(k)}{\sqrt{k^+}}\gamma^\mu\frac{u(l)}{\sqrt{l^+}} \quad , \quad g\frac{\bar{u}(k)}{\sqrt{k^+}}\gamma^\mu\frac{v(l)}{\sqrt{l^+}} \quad , \quad -g\frac{\bar{v}(k)}{\sqrt{k^+}}\gamma^\mu\frac{u(l)}{\sqrt{l^+}} \quad , \quad g\frac{\bar{v}(k)}{\sqrt{k^+}}\gamma^\mu\frac{v(l)}{\sqrt{l^+}} \,,$$

   where g is the corresponding coupling constant. For internal lines, sum over the spins. This sum gives the usual propagator that is used in regular perturbation rules, so in this convention, one should not introduce propagators for internal fermion lines, as some other conventions do (as for example, reference [26]), except for the instantaneous propagators that we will discuss below. The factors $1/\sqrt{k^+}$ and/or $1/\sqrt{l^+}$ are omitted for external lines.

5. For each intermediate state write a factor

$$\frac{1}{\sum_{inc} k^- - \sum_{interm} k^- + i\varepsilon} \,,$$

   where the sums are over al the minus components of the momenta of the incident and intermediate particles.

6. The fermion propagators have instantaneous parts, $\gamma^+/(2k^+)$, but the instantaneous part can be absorbed in the regular propagator $\frac{\not{k}+m}{k^2-m^2}$ (that arises each time a $\sum_{spins} u(k)\bar{u}(k)$ appears because of rule 4) by replacing the numerator of each propagator that extend over only a single time interval with $\tilde{\not{k}} + m$, where

$$\tilde{k} = (k^+, \sum_{inc} k^- - \sum_{interm} k^-, \mathbf{k_T}) \,.$$

   The same replacement can be used of course for $\not{k} - m$ and $\sum_{spins} v(k)\bar{v}(k)$.

7. Integrate over dk^+ and $d\mathbf{k_T}/(16\pi^3)$ for each undetermined momentum and sum over all internal spins and polarizations.

6.1.3 The method of integrating over the minus components of momenta

As already mentioned, there are examples where the integration over the minus components of momenta give the same results as light cone perturbation techniques [25] [27]. It will be very illustrative to follow this technique, and combine it with rule number 6 to obtain the color dipole model. Let's start by analyzing the scattering of a weak charged

axial current off the target as an example. At small Bjorken variable x and at high energies, the main contribution to the process comes from diagrams as the one shown in figure 6.1, where the virtual boson fluctuates in a quark-antiquark pair, which scatters off the target. We only consider up and down quarks with masses m and d respectively. There are 5 more diagrams that are obtained by changing the place where we connect the gluon lines, and by inverting the direction of the fermion lines, but they all give similar contributions so we will concentrate in analyzing the one of figure 6.1. In the virtual boson-dipole vertex we have a $\gamma_\mu\gamma_5$ vertex, and in the dipole-pion vertex we put a γ_5 vertex.

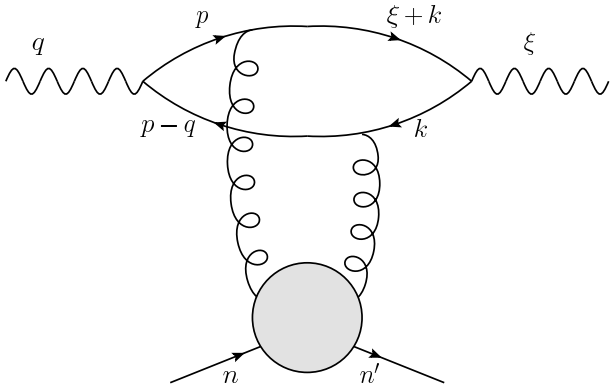

Figure 6.1: **One of the six diagrams contributing to the process**

The Feynman amplitude for the process is

$$\mathcal{M} = A^\mu \mathcal{M}_\mu \,, \tag{6.5}$$

where A^μ is a part of the process that is not interesting to us right now, and

$$\mathcal{M}_\mu = \kappa \int \frac{d^4k}{(2\pi)^4}\frac{d^4p}{(2\pi)^4} T^{ab} \left(\frac{\not\xi + \not k + m}{(\xi+k)^2 - m^2}\gamma_a \frac{\not p + m}{p^2-m^2}\gamma_\mu\gamma_5 \frac{\not p - \not q + d}{(p-q)^2-d^2}\gamma_b \frac{\not k + d}{k^2-d^2}\gamma_5 \right) , \tag{6.6}$$

where κ is a constant and T^{ab} is a complicated tensor that represents the interaction of the two gluons with the target. Using

$$d^4p = \frac{1}{2}dp^+dp^-d^2\mathbf{p_T} \quad , \quad d^4p = \frac{1}{2}dk^+dk^-d\mathbf{k_T} \,, \tag{6.7}$$

we can integrate over the minus component of momenta. Note that we have several poles in p^- and k^- coming from the denominators of the propagators in the trace. When we integrate using the residue theorem, we have to choose a contour that include some of these poles.

Let's analyze the poles in

$$\frac{1}{p^2-m^2}\cdot\frac{1}{(p-q)^2-d^2} = \frac{1}{p^+(p-q)^+}\frac{1}{p^- - \frac{\mathbf{p_T}^2}{p^+} - \frac{m^2}{p^+} + \frac{i\varepsilon}{p^+}} \cdot \frac{1}{(p-q)^- - \frac{(\mathbf{p_T}-\mathbf{q_T})^2}{(p-q)^+} - \frac{d^2}{(p-q)^+} + \frac{i\varepsilon}{(p-q)^+}} . \tag{6.8}$$

Note that if we use $(p-q)^+ = (z-1)q^+$ and $p^+ = zq^+$, we see that only with $z \in [0,1]$ the poles of p^- have different signs, i.e., one lies above the real axis and the other below, as in figure 6.2, so if we close the contour of integration from above or from below, we always

get a non vanishing result. If z lies outside $[0,1]$, both poles are above or below the axis, so closing the contour from below or above the axis respectively, we get a vanishing result for the integral. The same thing happens with the integral over d^4k. Then, integrating over p^- and k^- and picking the poles in $p^- = (\mathbf{p_T}^2 + m^2)/p^+$ and $k^- = (\mathbf{k_T}^2 + d^2)/p^+$ we obtain

$$\mathcal{M}_\mu = \kappa \sum_{\lambda_1,\lambda_2,\lambda_3,\lambda_4} \int \frac{d^2\mathbf{k_T}dk^+}{(2\pi)^3}\frac{d^2\mathbf{p_T}dp^+}{(2\pi)^3} T^{ab}\bar{v}_{\lambda_1}(-k)\gamma_5 u_{\lambda_2}(\xi+k) \tag{6.9}$$

$$\cdot\bar{u}_{\lambda_2}(\xi+k)\gamma_a u_{\lambda_3}(p)\bar{u}_{\lambda_3}(p)\gamma_\mu\gamma_5 v_{\lambda_4}(p-q)\bar{v}_{\lambda_4}(p-q)\gamma_b v_{\lambda_1}(-k) \tag{6.10}$$

$$\cdot\frac{1}{p^+(q-p)^+}\cdot\frac{1}{q^- - (p^- + \frac{(\mathbf{q_T}-\mathbf{p_T})^2}{(q-p)^+} + \frac{d^2}{(q-p)^+})} \tag{6.11}$$

$$\cdot\frac{1}{k^+(\xi+k)^+}\cdot\frac{1}{\xi^- + k^- - \frac{(\xi_\mathbf{T}+\mathbf{k_T})^2}{(\xi+k)^+} - \frac{m^2}{(\xi+k)^+}}\,. \tag{6.12}$$

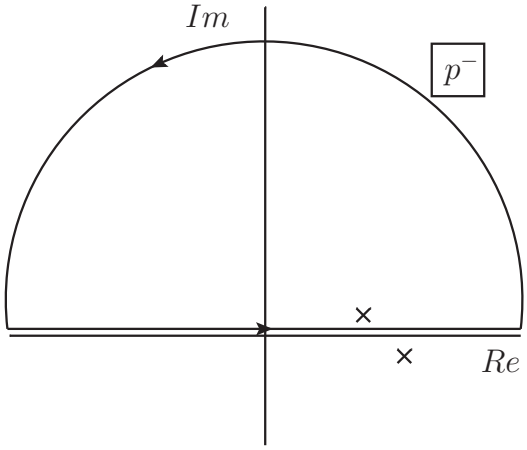

Figure 6.2: **Contour of integration**

Note that because of our choice of poles, the spinor's variables p and k are *on shell*. We define a function χ and the wave functions of the W boson and pion as (we write only the dependence of the transverse momenta in the WF, and we assume implicitly that they also depend on the other components of momenta and helicities)

$$\chi(k_T,p_T) = \kappa\frac{\xi^+}{(2\pi)^3}\frac{q^+}{(2\pi)^3}\frac{T^{ab}\bar{u}_{\lambda_2}(\xi+k)\gamma_a u_{\lambda_3}(p)\bar{v}_{\lambda_4}(p-q)\gamma_b v_{\lambda_1}(-k)}{\sqrt{p_1^+ p_2^+ p_1^{'+} p_2^{'+}}} \tag{6.13}$$

$$\Psi^\pi_{q\bar{q}}(\mathbf{k_T}) = \frac{(\bar{v}_{\lambda_1}(-k)\gamma_5 u_{\lambda_2}(\xi+k))^*}{\sqrt{p_1^{'+}}\sqrt{p_2^{'+}}(q^- - p_1^{'-} - p_2^{'-})} \tag{6.14}$$

$$\Psi^{W_A}_{q\bar{q}}(\mathbf{p_T}) = \frac{\bar{u}_{\lambda_3}(p)\varepsilon^\mu\gamma_\mu\gamma_5 v_{\lambda_4}(p-q)}{\sqrt{p_1^+}\sqrt{p_2^+}(q^- - p_1^- - p_2^-)}\,, \tag{6.15}$$

so that 6.12 can be written as (dropping the $q\bar{q}$ subindexes in the WF)

$$\mathcal{M}_h = \sum_{\lambda_1,\lambda_2,\lambda_3,\lambda_4}\int d^2\mathbf{k_T}dz'd^2\mathbf{p_T}dz\Psi^*_\pi(\mathbf{k_T})\chi(\mathbf{k_T},\mathbf{p_T})\Psi_{W_A}(\mathbf{p_T})\,. \tag{6.16}$$

Now, there is one difference between the WF that we define here and the ones defined in 3.21 : in 6.15 only one of the two spinors is on-shell, and the other one is calculated from energy-momentum conservation. If we recall rule number 6 from the LCPR, putting one of the propagators off shell (the one that extends over only a single time interval) is precisely the prescription needed to include the instantaneous propagators in the calculations. But the instantaneous propagators at high energies are suppressed in the scattering amplitude by a power of the c.m. energy, so we can neglect them and put both quarks on shell. *Much care is needed in this step*, as for moderate values of the c.m. energy, (less than one GeV), this assumption cannot be made.

We have been successful in arriving to the expression 3.21 provided that we make the identification $\chi(k_T, p_T) = \langle q\bar{q}(\mathbf{k_T}, \mathbf{\Delta}, z', q'^+, \lambda_1', \lambda_2') \mid \hat{D} \mid q\bar{q}(\mathbf{p_T}, z, q^+, \lambda_1, \lambda_2)\rangle$. We obtained this result using a purely mathematical treatment using the Feynman rules, without the use of the diffraction formalism. Going to configuration space by using

$$\chi(\mathbf{k_T}, \mathbf{p_T}) = \int d^2\mathbf{r_T} d^2\mathbf{r'_T} \exp\left(i\mathbf{k_T}\cdot\mathbf{r'_T}\right) \exp\left(-i\mathbf{p_T}\cdot\mathbf{r_T}\right)\chi(\mathbf{r_T}, \mathbf{r'_T})\,, \tag{6.17}$$

we obtain

$$\mathcal{M}_h = \sum_{\lambda_1,\lambda_2,\lambda_3,\lambda_4} \int d^2\mathbf{r_T} dz' d\mathbf{r'_T} dz \Psi_\pi^*(\mathbf{r'_T})\chi(\mathbf{r'_T}, \mathbf{r_T})\Psi_{W_A}(\mathbf{r_T})\,. \tag{6.18}$$

This result can be interpreted as follows. Before scattering off the target, the W boson fluctuates into a quark-antiquark dipole. The amplitude of that process is given by the W boson dipole wave function. This color dipole then scatters off the target with an amplitude $\chi(\mathbf{r_T}, \mathbf{r'_T})$, and changes its transverse size $\mathbf{r_T}$ and light cone momentum fraction z to $\mathbf{r'_T}$ and z'. To obtain the color dipole model only one further assumption is needed, that the transverse size of the dipole does not change, i.e., it remains *frozen* as it scatters off the target. This can be understood by analyzing the lifetime of the color dipole. The dipole energy is

$$E_{q\bar{q}} = \frac{1}{2}\left(q^+ + \frac{\mathbf{k_T}^2 + m^2}{zq^+} + \frac{\mathbf{k_T}^2 + d^2}{(1-z)q^+}\right)\,. \tag{6.19}$$

Then, the uncertainty between the W boson energy and the dipole energy is,

$$\Delta E = \frac{1}{2q^+}\left(Q^2 + \frac{\mathbf{k_T}^2 + m^2(1-z) + d^2 z}{z(1-z)}\right)\,, \tag{6.20}$$

so that the dipole lifetime is

$$\tau = \frac{1}{\Delta E} = \frac{2q^+}{Q^2 + \frac{\mathbf{k_T}^2 + m^2(1-z) + d^2 z}{z(1-z)}}\,. \tag{6.21}$$

If we review the wave functions given in 4.2.1, we see that at high Q^2 they filter the values of $\mathbf{k_T}$ greater than $Q^2 z(1-z)$. Then, we can use $\tau \approx \frac{q^+}{Q^2} \propto \frac{1}{m_N x}$, where m_N is the target mass. Then, for small values of x, this lifetime is big in comparison to the time in which the scattering occurs $\approx r_N$, where r_N is the target radius, so that we can think that the dipole travels through the target with a fixed transverse size. This is equivalent to think that the dynamics at which the dipole can change its transverse size is much slower than the dynamics at which the scattering occurs.

6.2 Appendix II: optics, non relativistic Q.M. and Glauber's model

In section 4.2.1 we studied the perturbative wave functions of the W boson and pion. The second important quantity in the dipole model is the dipole scattering amplitude, $\mathcal{A}$. Let's recall equation 3.24

$$\mathcal{M}_h = \sum_{\lambda_1,\lambda_2,\lambda_1',\lambda_2'} \int d^2\mathbf{r_T} dz dz' \cdot \Psi_\pi^*(\mathbf{r_T}, z', m_\pi^2, q_+', \lambda_1', \lambda_2') \Psi_W(\mathbf{r_T}, z, Q^2, q_+, \lambda_1, \lambda_2) \mathcal{A}(r_T, q_+, q_+', z, z', \lambda_1, \lambda_2, \lambda_1', \lambda_2') \,.$$

In this appendix we will study this scattering amplitude in the context of dipole-nuclei scattering, *i.e*, multiple scattering of dipoles by several nucleons. To obtain our results, we will start from a non-relativistic quantum mechanical treatment, and we will study the non-relativistic scattering amplitude f using Glauber's theory.

The first assumption that we are going to make, is that the scattering amplitude will depend only on the transverse separation of the dipoles and the c.m. transverse momentum transferred to the dipole, $\mathbf{\Delta}$. We will also allow a dependence on the boson energy ν, virtuality q^2 and the c.m energy s' (see figure 2.1), but to simplify the notation we will write

$$f(r_T, q_+, q_+', z, z', \lambda_1, \lambda_2, \lambda_1', \lambda_2') = f(r_T, \mathbf{\Delta}) \,. \tag{6.22}$$

Taking the Fourier transform we have

$$f(r_T, \mathbf{\Delta}) = \int d^2\mathbf{b} \exp\left(-i\mathbf{\Delta}\cdot\mathbf{b}\right) f(r_T, \mathbf{b}) \,, \tag{6.23}$$

where $\mathbf{b}$ is called the *impact parameter*. The approach that we are going to use to solve the problem comes from optics and non-relativistic quantum mechanics. In optics, the scattering amplitude of a plane wave with wave vector $\mathbf{k}$ that scatters off an object is given by

$$f_{opt}(\Delta) = \frac{ik}{2\pi} \int d^2\mathbf{b} \exp\left(-i\mathbf{\Delta}\cdot\mathbf{b}\right) \Gamma_{opt}(\mathbf{b}) \,, \tag{6.24}$$

where $\mathbf{\Delta}$ is the momentum transferred to the wave in the plane transverse to $\mathbf{k}$, and Γ_{opt} is the *profile function* of the object. The scattering cross section is simply

$$\frac{d\sigma}{d\Omega} = |f(\mathbf{\Delta})|^2 \,. \tag{6.25}$$

The profile function is a very useful quantity. It gives us an intuitive view of the target, as it represents how big is it in the transverse plane. For example, the profile function

$$\Gamma_{opt}(b) = \begin{cases} constant & b \le R \\ 0 & b > R \end{cases} \,, \tag{6.26}$$

corresponds to a black disk of radius R. These concepts taken from optics were first used in non-relativistic Q.M., and then adapted to relativistic quantum field theories.

In non-relativistic quantum mechanics, at high energies the *eikonal approximation* [23] is valid. In this approximation, the scattering amplitude can be written as

$$f(\mathbf{\Delta}) = \frac{ik}{2\pi} \int d^2\mathbf{b} \exp\left(-i\mathbf{\Delta}\cdot\mathbf{b}\right) \int \left(\prod_{i=1}^{A} d\mathbf{r}_i\right) |\Psi(\{\mathbf{r}_i\})|^2 \big(1 - \exp(i\chi_A(\mathbf{b}, \{\mathbf{b_i}\}))\big) \,, \tag{6.27}$$

where $\Psi(\{\mathbf{r}_i\})$ is the nuclear wave function, $\{\mathbf{b_i}\} = (\mathbf{b_1}, \mathbf{b_2}..\mathbf{b_A})$ is the set of vectors that define the position of each nucleon in the transverse plane and $\chi_A(\mathbf{b}, \{\mathbf{b_i}\})$ is the phase shift that the matter wave suffers when it scatters off the target and is given by

$$\chi_A(\mathbf{b}, \{\mathbf{b_i}\}) = -\frac{1}{2k} \int_{-\infty}^{\infty} V_A(\mathbf{b}, \{\mathbf{b_i}\}, z) dz \,. \tag{6.28}$$

$V_A(\mathbf{b}, \{\mathbf{b_i}\}, z)$ is the classical potential that represents the nucleus. If the nucleons are uncorrelated, the nuclear potential is just the sum of the one-nucleon potentials,

$$V_A(\mathbf{b}, \{\mathbf{b_i}\}, z) = \sum_{i=1}^{A} V_i(\mathbf{b} - \mathbf{b_i}, \mathbf{z}) \,, \tag{6.29}$$

so that the phase shift is also just the sum of the phase shifts contributed by the individual nucleons

$$\chi_A(\mathbf{b}, \{\mathbf{b_i}\}) = \sum_{i=1}^{A} \chi_i(\mathbf{b} - \mathbf{b_i}, \mathbf{z}) \,. \tag{6.30}$$

Now, in analogy to optics, we define the optical phase and the profile function

$$\Gamma_{opt} = 1 - \exp(i\chi_{opt}(\mathbf{b}) = \int \left(\prod_{i=1}^{A} d\mathbf{r}_i \right) |\Psi(\{\mathbf{r}_i\})|^2 \big(1 - \exp(i\chi_A(\mathbf{b}, \{\mathbf{b_i}\}))\big) \,, \tag{6.31}$$

so that equation 6.24 represents again the scattering amplitude, now of a particle scattering off a nucleus. We also define the profile function of each nucleon

$$\Gamma_i = 1 - \exp(i\chi_i(\mathbf{b} - \mathbf{b_i}, \mathbf{z})) \,, \tag{6.32}$$

which can be obtained using the general expression 6.28 for the case of $A = 1$ but normally a Gaussian parametrization is used instead. Inserting 6.32 in 6.31 and using 6.30 we obtain

$$\begin{aligned} \Gamma_{opt} &= \int \left(\prod_{i=1}^{A} d\mathbf{r}_i \right) |\Psi(\{\mathbf{r}_i\})|^2 \Big(1 - \prod_{i=1}^{A} (1 - \Gamma_i)\Big) \\ &= 1 - \int \left(\prod_{i=1}^{A} d\mathbf{r}_i \right) |\Psi(\{\mathbf{r}_i\})|^2 \prod_{i=1}^{A} (1 - \Gamma_i) \,. \end{aligned} \tag{6.33}$$

If the wave functions are uncorrelated so that $\Psi(\{\mathbf{r}_i\}) = \prod_{i=1}^{A} \Psi_i(\mathbf{r}_i)$ we obtain

$$\Gamma_{opt} = 1 - \prod_{i=1}^{A} \Big(1 - \int d\mathbf{r_i} |\Psi_i(\mathbf{r}_i)|^2 \Gamma_i\Big) \,. \tag{6.34}$$

To simplify this expression, we can think that the nucleus is an object with density $n_A(\mathbf{r})$, composed by identical nucleons centered at the nucleus origin with profile function Γ. Each nucleon contributes with a density $n_N = \frac{n_A(\mathbf{r})}{A}$ to the nuclear density. $n_A(\mathbf{r})$ is normalized according to

$$\int_{-\infty}^{\infty} dz \int d^2\mathbf{b}' n_A(\mathbf{r}') = A \,, \tag{6.35}$$

so that n_N is normalized to unity and can be used as the nucleon wave function. In this way, 6.34 reduces to

$$\Gamma_{opt} = 1 - \Big(1 - \frac{1}{A} \int d^2\mathbf{b}' \Gamma(\mathbf{b} - \mathbf{b}') \int n_A(\mathbf{b}', z) dz\Big)^A \,. \tag{6.36}$$

As already mentioned, usually a Gaussian parametrization is used for the nucleon profile function. In our case, where we study the scattering of a dipole off nuclei, we use

$$\Gamma(\mathbf{b} - \mathbf{b}') = \frac{\sigma^p_{q\bar{q}}(\mathbf{r_T})(1 - i\rho_{q\bar{q}N})}{4\pi B} \exp\left(-\frac{(\mathbf{b} - \mathbf{b}')^2}{2B}\right) \,, \tag{6.37}$$

where $\sigma^p_{q\bar{q}}(\mathbf{r_T})$ is the dipole-nucleon cross section, $\rho_{q\bar{q}N}$ is the ratio of the real to imaginary parts of the forward elastic $q\bar{q}N$ scattering amplitude which is very small at high energies, so we will neglect it, and B is the slope of the Gaussian that represents the nucleon. Defining the nuclear optical thickness

$$T(\mathbf{b}') = \int_{-\infty}^{\infty} dz n_A(\mathbf{b}', z) \tag{6.38}$$

and

$$\tilde{T}(\mathbf{b}) = \frac{1}{2\pi B} \int d^2\mathbf{b}' T(\mathbf{b}') \exp\left(-\frac{(\mathbf{b}-\mathbf{b}')^2}{2B}\right), \tag{6.39}$$

we obtain

$$\Gamma_{opt} = 1 - \left(1 - \frac{1}{2A}\sigma^p_{q\bar{q}}(\mathbf{r_T})\tilde{T}(\mathbf{b})\right)^A. \tag{6.40}$$

Now, it is reasonable to assume that the slope B is much smaller than the nuclear radius squared, because Γ represents the profile function of a nucleon. Then, we can approximate $\tilde{T}(\mathbf{b}) \approx T(\mathbf{b})$ and we finally get

$$f(\mathbf{\Delta}) = \frac{ik}{2\pi} \int d^2\mathbf{b} \exp\left(-i\mathbf{\Delta}\cdot\mathbf{b}\right) \left(1 - \left(1 - \frac{1}{2A}\sigma^p_{q\bar{q}}(\mathbf{r_T})T(\mathbf{b})\right)^A\right). \tag{6.41}$$

To use this result in relativistic theories, we have to find a relation between the classical scattering amplitude f and the relativistic Feynman amplitude $\mathcal{A}$. This can be achieved by comparing the formulas for the scattering cross sections for f and $\mathcal{A}$ for the scattering of two particles [3],

$$\frac{d\sigma}{d\Omega} = |f(\mathbf{\Delta})|^2 \quad , \quad \frac{d\sigma}{d\Omega} = \frac{\sqrt{\lambda(s, m_3^2, m_4^2)}}{64\pi^2 s\sqrt{\lambda(s, m_1^2, m_2^2)}}|\mathcal{A}|^2, \tag{6.42}$$

where λ is the triangle function, m_1 and m_2 are the masses of the incoming particles, m_3 and m_4 of the final particles and s is the center of mass energy. The momentum k appearing in 6.41 must be interpreted as the momentum of one of the particles in the c.m. system, so it is given by

$$k = \frac{\sqrt{\lambda(s, m_1^2, m_2^2)}}{2\sqrt{s}}. \tag{6.43}$$

Comparing both amplitudes in 6.42 we see that

$$|\mathcal{A}|^2 = 4\sqrt{\frac{\lambda(s, m_1^2, m_2^2)^3}{\lambda(s, m_1^2, m_2^2)}} \left| \int d^2\mathbf{b} \exp\left(-i\mathbf{\Delta}\cdot\mathbf{b}\right) \left(1 - \left(1 - \frac{1}{2A}\sigma^p_{q\bar{q}}(\mathbf{r_T})T(\mathbf{b})\right)^A\right) \right|^2. \tag{6.44}$$

In section 3.3, this formula is used for a dipole that scatters off nuclei. The dipole itself has no definite "mass", as it is an eigenstate of transverse separation and not of momentum, but we can take its "mass" to be the virtuality of the W boson, q^2. In the same way, we will use m_π^2 for the squared mass of the final dipole. Then, the scattering amplitude of the dipole is given by

$$|\mathcal{A}|^2 = 4\sqrt{\frac{\lambda(s', q^2, m_N^2)^3}{\lambda(s', m_\pi^2, m_N^2)}} \left| \int d^2\mathbf{b} \exp\left(-i\mathbf{\Delta}\cdot\mathbf{b}\right) \left(1 - \left(1 - \frac{1}{2A}\sigma^p_{q\bar{q}}(\mathbf{r_T})T(\mathbf{b})\right)^A\right) \right|^2. \tag{6.45}$$

But for heavy nuclei, $m_N \approx 200[GeV]$, the mass of the pion and q^2 are much smaller than s' and m_N so they can be neglected, and we can approximate $\lambda(s', m_\pi^2, m_N^2) \approx \lambda(s', 0, m_N^2)$

and $\lambda(s', q^2, m_N^2) \approx \lambda(s', 0, m_N^2)$, so $\lambda(s', m_\pi^2, m_N^2) \approx \lambda(s', q^2, m_N^2)$. Then, the amplitude reduces to

$$\mathcal{A} = 2\lambda(s', q^2, m_N^2) \int d^2\mathbf{b} \exp\left(-i\mathbf{\Delta}\cdot\mathbf{b}\right) \left(1 - \left(1 - \frac{1}{2A}\sigma_{q\bar{q}}^p(\mathbf{r_T})T(\mathbf{b})\right)^A\right), \tag{6.46}$$

up to a complex phase. For big values of A, the terms inside the brackets can be approximated by an exponential. Note that if we expand the term inside the parenthesis using the binomial theorem, we get a sum over powers of $\sigma T(b)$. The first power in this sum represents the scattering of the dipole on A nucleons. The second and higher order terms represent the shadowing corrections.

6.3 Appendix III: conventions for the gamma matrices and spinors

We follow the conventions of [24] for the gamma matrices and spinors.

Gamma Matrices

$$\gamma_0 = \begin{pmatrix} 1 & 0 & 0 & 0 \\ 0 & 1 & 0 & 0 \\ 0 & 0 & -1 & 0 \\ 0 & 0 & 0 & -1 \end{pmatrix}, \tag{6.47}$$

$$\gamma_i = \begin{pmatrix} 0 & \sigma_i \\ -\sigma_i & 0 \end{pmatrix}, \tag{6.48}$$

$$\gamma_5 = i\gamma_0\gamma_1\gamma_2\gamma_3, \tag{6.49}$$

σ_i, $i = 1, 2, 3$ are the Pauli matrices,

$$\sigma_1 = \begin{pmatrix} 0 & 1 \\ 1 & 0 \end{pmatrix} \quad , \quad \sigma_2 = \begin{pmatrix} 0 & -i \\ i & 0 \end{pmatrix} \quad , \quad \sigma_3 = \begin{pmatrix} 1 & 0 \\ 0 & -1 \end{pmatrix}. \tag{6.50}$$

.

Light cone Gamma Matrices

$$\gamma^+ = \gamma_0 + \gamma_3, \tag{6.51}$$

$$\gamma^- = \gamma_0 - \gamma_3. \tag{6.52}$$

Light cone spinors of momentum p

$$u(\lambda = \frac{1}{2}) = \frac{1}{\sqrt{p^+}}(p^+ + \beta m + \boldsymbol{\alpha}_T\mathbf{p}_T)\chi_\uparrow, \tag{6.53}$$

$$u(\lambda = -\frac{1}{2}) = \frac{1}{\sqrt{p^+}}(p^+ + \beta m + \boldsymbol{\alpha}_T\mathbf{p}_T)\chi_\downarrow, \tag{6.54}$$

$$v(\lambda = \frac{1}{2}) = \frac{1}{\sqrt{p^+}}(p^+ - \beta m + \boldsymbol{\alpha}_T\mathbf{p}_T)\chi_\downarrow, \tag{6.55}$$

$$v(\lambda = -\frac{1}{2}) = \frac{1}{\sqrt{p^+}}(p^+ - \beta m + \boldsymbol{\alpha}_T\mathbf{p}_T)\chi_\uparrow, \tag{6.56}$$

where

$$\chi_{\uparrow} = \frac{1}{\sqrt{2}} \begin{pmatrix} 1 \\ 0 \\ 1 \\ 0 \end{pmatrix}, \tag{6.57}$$

$$\chi_{\downarrow} = \frac{1}{\sqrt{2}} \begin{pmatrix} 0 \\ 1 \\ 0 \\ -1 \end{pmatrix}. \tag{6.58}$$

References

[1] B.Z.Kopeliovich and P.Marage, *"Low Q^2, high neutrino nu physics (CVC, PCAC, hadron dominance)"*, Int. J. Mod. Phys. A **8**, 1513 (1993).

[2] J. S. Bell, Mary Bell, Kurt Gottfried, Martinus Veltman, *"Quantum mechanics, high energy physics and accelerators: selected papers of John S.Bell"* (World Scientific Publishing, 1995).

[3] Barone, Predazzi, *"High-Energy Particle Diffraction"* (Springer, 2002).

[4] Fiore, Zoller, *"Color Dipoles, PCAC, and Adler's Theorem"*, JETP Letters, 2007, **85**, No. 7, pp. 309–314 (2007).

[5] M.L. Good and W.D. Walker, *"Diffraction Dissociation of Beam Particles"*, Phys. Rev. **120**,1857 (1960).

[6] B.Z. Kopeliovich,I. Potashnikova and Ivan Schmidt, *Diffraction in QCD*, [arxiv:hep-ph/0604097]

[7] Peskin, Schroeder, *"An Introduction to Quantum Field Theory"* (Perseus, 1995).

[8] Stanley J. Brodsky, L. Frankfurt, J.F. Gunion, A.H. Mueller, M. Strikman, *"Diffractive leptoproduction of vector mesons ins QCD"*, Phys. Rev. D **50**, 3134 (1994).

[9] Al. B. Zamolodchikov, B.Z. Kopeliovich and L.I. Lapidus, *"Color dynamics in hadron diffraction by nuclei"*, Pis'ma Zh. Eksp. Teor. Fiz. **33**, No. 11, 612-614 (1981).

[10] G. Peter Lepage, Stanley J. Brodsky, *"Exclusive processes in perturbative quantum chromodynamics"*, Phys. Rev. D **22**, 2157 (1980).

[11] H. Kowalski and D. Teaneay *"Impact parameter dipole saturation model"*, Phys. Rev. D **68**, 114005 (2003).

[12] S. Munier , A.M. Stasto, A.H. Mueller, *Impact parameter dependent S-matrix for dipole–proton scattering from diffractive meson electroproduction*, Nucl. Physi. B **603** 427 (2001).

[13] Carlo Ewerz, Otoo Nachtmann, *Towards a Nonperturbative Foundation of the Dipole Picture: I. Functional Methods* [arXiv:hep-ph/0404254].

[14] Carlo Ewerz, Otoo Nachtmann, *Towards a Nonperturbative Foundation of the Dipole Picture: II. High Energy Limit* [arXiv:hep-ph/0604087].

[15] T. Frederico and G.A. Miller, *Null-plane phenomenolofy for the pion decay constant and radius*, Phys. Rev. D **45**, 4207 (1992).

[16] Boris Kopeliovich, Andreas Schäfer, Alexander Tarasov, *Nonperturbative effects in gluon radiation and photoproduction of quark pairs*, Phys. Rev. D **62**, 054022 (2000).

[17] B.Z. Kopeliovich, Ivan Schmidt and M. Siddikov, *DVCS via color dipoles: Nonperturbative effects* [arXiv:hep-ph/0812.3992v2].

[18] P. Marage *et al.* WA59 Collaboration, Zeitschrift für Physik C **31**, 191 (1986).

[19] Boris Kopeliovich, Bogdan Povh, *Scaling variable for nuclear shadowing in deep-inelastic scattering*, Phys. Lett. B, **367** 329-334 (1996).

[20] Boris Kopeliovich, Bogdan Povh, *Scaling variable for nuclear shadowing in deep-inelastic scattering*, Phys. Lett. B, **367** 329-334 (1996).

[21] B.Z. Kopeliovich, J. Nemchik, A. Schafer and A.V. Tarasov, *Color Transparency Versus Quantum Coherence in Electroproduction of Vector Mesons off Nuclei*, [arXiv:hep-ph/0107227].

[22] Mandl, Shaw, *"Quantum Field Theory"* (Wiley, 1984).

[23] R. J. Glauber, *"High Energy Collision Theory"*, presented at the Theoretical Physics Institute, University of Colorado, (1958).

[24] Stanley J. Brodsky, Hans-Christian Pauli, Stephen S. Pinsky, *Quantum chromodynamics and other field theories on the light cone*, Physics Reports **301** 299, (1998).

[25] Stanley J. Brodsky, Ralph Roskies, Roberto Suaya, *Quantum Electrodynamics and Renormalization Theory in the Infinite-Momentum Frame*, Phys. Rev. D **8** 4574, (1973).

[26] Alex Langnau, *Perturbation Theory in Light-Cone Quantization*, PhD thesis, SLAC-0385 (1992).

[27] Michael G. Schmidt *Simple connection between covariant Feynman formalism and time-ordered perturbation theory in the infinite-momentum frame*, Phys. Rev. D **9** 408, (1974).

[28] Alfredo Vega, Ivan Schmidt, Tanja Branz, Thomas Gutsche, Valery E. Lyubovitskij, *Meson wave function from holographic models*, Phys. Rev. D **80**, 055014 (2009).

[29] Avaroth Harinfranath, *An Introduction to Light-Front Dynamics for Pedestrians*, [arXiv:hep-ph/9612244].